AD-A141 460   A FESTSCHRIFT OF TECHNICAL PAPERS PRESENTED TO WILHELM   1/1
S ERICKSEN ON THE..(U) AIR FORCE INST OF TECH
WRIGHT-PATTERSON AFB OH B W WOODRUFF JAN 84
UNCLASSIFIED AFIT-EN-TM-84-1   F/G 5/2   NL

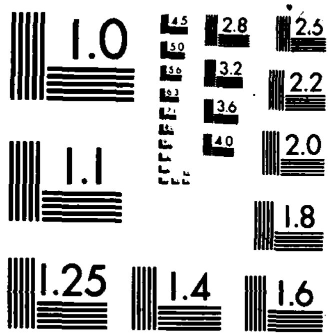

MICROCOPY RESOLUTION TEST CHART
NATIONAL BUREAU OF STANDARDS-1963 A

A FESTSCHRIFT OF TECHNICAL PAPERS
PRESENTED TO WILHELM S. ERICKSEN
ON THE OCCASION OF HIS JOINING
THE EMERITUS FACULTY OF THE
AIR FORCE INSTITUTE OF TECHNOLOGY

AFIT-EN-TM-84-1

Brian W. Woodruff
Captain USAF
Editor

Approved for public release; IAW AFR 190-17.

LYNN E. WOLAVER
Dean for Research and Professional Development
Air Force Institute of Technology (ATC)
Wright-Patterson AFB OH 45433

Foreword

Wilhelm Schelstadt Ericksen earned the Bachelor of Arts in Mathematics at St. Olaf College in 1936. He earned the Master of Arts in Mathematics at the University of Wisconsin in 1938. He was awarded the Ph.D. in mathematics at Wisconsin in 1943, with a dissertation on, "Asymptotic Forms of the Solutions of the Differential Equation for the Associated Mathieu Functions."

He began his college teaching career in 1942 at St. Olaf College, and he taught at Minot State Teachers' College for the academic year 1943-44. He was a Fellow in Mechanics at Brown University in 1944-45.

Dr. Ericksen worked as an aerodynamicist for Bell Aircraft in 1946, and in that year he also began a six-year association with the United States Forest Products Laboratory in Madison, Wisconsin. He joined the faculty of the United States Air Force Institute of Technology in 1953.

Professor Ericksen's long list of publications began with a series of Forest Products Laboratory reports on the behavior of sandwich panels under loads, and continues with recent articles in the Society for Industrial and Applied Mathematics' Journal on Numerical Analysis, on inverse pairs of matrices with integer elements.

Wilhelm Ericksen's teaching is characterized by scholarship of the highest degree, coupled with a caring and gentle concern for his students as human beings. These splendid qualities have endeared him to thirty academic generations of AFIT students and to his colleagues, who present these papers to him as tokens of their affection and esteem on the occasion of his joining the emeritus faculty.

D. A. Lee

December 1982

TABLE OF CONTENTS

THE PCT CONTROL SYSTEM DESIGN FOR SAMPLED-DATA CONTROL SYSTEMS

by

C. H. Houpis*

October 4, 1982

ABSTRACT

The pseudo-continuous-time (PCT) control system approximation of a sampled-data system permits the use of tried and proven continuous-time domain methods for designing cascade and/or feedback controllers. When the rules governing the use of the Pade approximation and the Tustin transformation are satisfied, the PCT design approach is a valuable technique for the design of sampled-data control systems.

*Professor of Electrical Engineering, School of Engineering,
Air Force Institute of Technology, Wright-Patterson AFB, Ohio 45433

I. Introduction

The analysis and design of sampled-data control systems may be done entirely in the z-plane, which is referred to as the direct digital control design (DIR) technique[2] or entirely in the s-plane. The latter is referred to as the digitization (DIG) technique which requires the development of the pseudo-continuous-time (PCT) system model. This model requires the use of the Padé and Tustin transformation approximations. A controller, $D_c(z)$ designed by the DIG technique provides a good base for exhibiting the effects of the sample time parameter of the digitized controller on the performance of the system. The reason for this is that the continuous controller corresponds to the limiting case where the sampling time of $D_c(z)$ is zero. A disadvantage of this method is that $D_c(z)$ may not have all the properties of $D_c(s)$. However, this problem is minimized by the selection of a s to z (to w) transformation algorithm which maintains the specified properties required of the controller. This paper develops the PCT control system model and the criteria for achieving a good correlation between the s- and z-plane mapping. If the degree of correlation is not satisfactory, then the DIG technique may permit the desired system performance characteristics to be achieved by mere gain adjustment in the z-domain.

II. Approximations

Tustin -- The Tustin s to z or z to s transformation is defined as

$$s = \frac{2}{T}\left(\frac{z-1}{z+1}\right) \tag{1}$$

or

$$z = \frac{1+sT/2}{1-sT/2} \tag{2}$$

and the exact z-transformation is defined as

$$z = \epsilon^{-sT} \tag{3}$$

By substituting $s = j\omega_{sp}$ into (2) and $s = j\hat{\omega}_{sp}$ into (3), where $\hat{\omega}_{sp}$ is an equivalent s-plane frequency, then equating the two expressions results in

$$\tan(\hat{\omega}_{sp}T/2) = \omega_{sp}T/2 \tag{4}$$

When $\hat{\omega}_{sp}T/2 \leq 0.3057$ rad (17^{o}) then

$$\hat{\omega}_{sp} \doteq \omega_{sp} \tag{5}$$

In a similar manner, substituting the exponentional series for $z = \epsilon^{-\hat{\sigma}_{sp}T}$ and $s = \sigma_{sp}$ into (2) results in

$$1 + \hat{\sigma}_{sp}T + \frac{(\hat{\sigma}_{sp}T)^2}{2} + \ldots = 1 + [\sigma_{sp}T/(1-\sigma_{sp}T/2)] \tag{6}$$

If $1 >> |\hat{\sigma}_{sp}T/2|$ and $1 >> |\sigma_{sp}T/2|$, then

$$|\hat{\sigma}_{sp}| \doteq |\sigma_{sp}| << 2/T \tag{7}$$

With (5) and (7) satisfied, the shaded area in Fig. 1 represents the allowable location of the poles and zeros in the s-plane for a good Tustin transformation.

<u>Padé</u> -- Using the first-order Padé approximation, the transfer function of the zero-order-hold (Z-O-H) device is approximated, when the value of T is small enough[4], as follows:

$$G_{zo}(s) = \frac{1 - \epsilon^{-Ts}}{s} \approx \frac{2T}{Ts + 2} = G_{pa}(s) \tag{8}$$

III. Pseudo Continuous-Time Control System (PCT)

The DIG method of designing a sampled-data system, in the complex frequency s-plane, requires a satisfactory PCT model of the sampled-data system. In other words, for the sampled-data system of Fig. 2, the sampler and the Z-O-H units are approximated by a linear continuous-time unit, $G_A(s)$, as shown in Fig. 3(c). The DIG method requires that the dominant poles and zeros of the PCT model must lie in the shaded area of Fig. 1 for a high level of correlation with the sampled-data system. To determine $G_A(s)$ first note that the frequency component of $E^*(j\omega)$, representing the continuous-time signal $E(j\omega)$ and all of its side-bands, is multiplied by $1/T$ [1,2]. Because of the low-pass filtering characteristics of a sampled-data system, only the primary component needs to be considered in the analysis of the system. Therefore, the PCT approximation of the sampler and the Z-O-H of Fig. 3(a) is shown in Fig. 3(b) where the Padé approximation, $G_{pa}(s)$, is used to replace $G_{zo}(s)$. Therefore, the sampler and Z-O-H units of a sampled-data system are approximated in the PCT system of Fig. 3(c) by the transfer function

$$G_A(s) = \frac{1}{T} G_{pa}(s) = \frac{2}{Ts + 2} \tag{9}$$

Since $\lim_{T \to 0} [G_A(s)] = 1$, (9) is an accurate PCT representation of the sampler and Z-O-H units, satisfying the requirement that as $T \to 0$ the output of $G_A(s)$ must equal its input. Further note that in the frequency domain, as $\omega_s \to \infty$ $(T \to 0)$, the primary strip in the s-plane becomes the entire frequency spectrum domain which is the representation for the continuous-time system.

Note that in obtaining PCT systems for the sampled-data systems of Fig. 4, the factor 1/T replaces only the sampler that is sampling the continuous-time signal. The sampler on the output of the digital controller is replaced by a factor of one. To illustrate the effect of the value of T on the validity of the results obtained by the DIG method, consider the sampled-data closed-loop control system of Fig. 2 where

$$G_x(s) = \frac{4.2}{s(s+1)(s+5)}$$

The closed-loop system performance for three values of T and $\zeta = 0.45$ are determined in both the s- and z- domains, i.e., the DIG and DIR methods, respectively. Table 1 presents the required value of K_x and time response characteristics for each value of T. Note that for $T \le 0.1$ there is a high correlation between the DIG and DIR models. For $T \leq 1$ there is still a relatively good correlation. (The designer needs to specify, for a given application, what is considered to be "good correlation.") The figures of merit of the corresponding continuous-time control system

$$\frac{C(s)}{R(s)} = \frac{G_x(s)}{1+G_x(s)} \tag{10}$$

for a unit-step forcing function are: $M_p = 1.202$, $t_p = 4.12$ sec and $t_s = 9.48$ sec.

Table 1 Performance Characteristics of a Sampled-data Control System using the DIR and DIG Methods

Method	T,sec	K_x	M_p	t_p,sec	t_s,sec
DIR	0.01	4.147	1.202	4.16	9.53
DIG		4.215	1.206	4.11	9.478
DIR	0.1	3.892	1.202	4.25	9.8^+
DIG		3.906	1.203	4.33^-	9.90^+
DIR	1	2.4393	1.2	6	13^+
DIG		2.496	1.200	6.18	13.76

IV. DIG Technique

Figure 5 represents the trial and error design philosophy in applying the DIG technique. If path A does not result in the specifications being met by the sampled-data control system of Fig. 4, then path B is used to try to determine a satisfactory value of K_{zc}. A similar chart may be drawn for the design of the feedback controller of Fig. 4(b). The design philosophy involves the following considerations:

(a) Follow path A if the dominant poles and zeros of $C(\cdot)/R(\cdot)$ lie in the shaded area of Fig. 1 (Tustin approximation is good!).

(b) Follow path A when the degree of warping is deemed not to negatively affect the achievement of the desired design results. If the desired results are not achieved, try path B.

(c) Follow path B when severe warping exists. The DIG design procedure is as follows:

Step 1 Convert the basic sampled-data control system to a PCT control system or transform the basic system into the w-plane (use both for design purposes).

Step 2 By means of a root-locus analysis or by use of the Guilleman-Truxal method determine $D_c(s) = K_{sc}D_c'(s)$ or $D_c(w) = K_{ws}D_c'(w)$.

Step 3 Obtain the control ratio of the compensated system and the corresponding time response for the desired forcing function. (This step is not necessary if the exact Guillemin-Truxal compensator is used.) If the desired performance results are not achieved, repeat Step 2 by selecting a different value of ζ, σ, ω_d, etc. or a different desired control ratio.

Step 4 When an acceptable $D_c(s)$ or $D_c(w)$ has been achieved, transform the compensator, via the Tustin transformation, into the z-domain.

Step 5 Obtain the z-domain control ratio of the compensated system and the corresponding time response for the desired forcing function. If the desired performance results for the sampled-data control system are achieved via path A or path B, then the design of the compensator is complete. If not, return to Step 2 and repeat the steps with a new compensator design or proceed to the DIR technique.

V. DIR Technique

The simple lead ($\alpha < 1$) and lag ($\alpha > 1$) compensators in the s-domain have the form

$$D_c(s) = \frac{K_{sc}(s - z_s)}{(s - p_s)} \tag{11}$$

where $p_s = z_s/\alpha$. The s-plane zero and pole are transformed into the z-domain as follows:

$$z_z = \epsilon^{sT}\Big|_{s=z_s} = \epsilon^{z_s T} \tag{12}$$

$$p_z = \epsilon^{sT}\Big|_{s=p_s} = \epsilon^{p_s T} = \epsilon^{z_s T/\alpha} \tag{13}$$

Thus, the corresponding first-order z-domain compensator (digital filter) is

$$D_c(z) = \frac{K_{zc}(z - z_z)}{z - p_z} = \frac{K_{zc}(z - z_z)}{z - z_z/\beta} \tag{14}$$

where $p_z = z_z/\beta$.

By taking the natural log of (12) and (13) a relationship between α and β is obtained as follows:

$$z_s T = \ln z_z \tag{15}$$

$$z_s T/\alpha = \ln p_z \tag{16}$$

Taking the ratio of these equations and rearranging yields $\alpha \ln p_z = \ln z_z$. Thus

$$p_z^{\alpha} = z_z \tag{17}$$

$$\beta = z_z/p_z = p_z^{\alpha-1} \tag{18}$$

For a lead network, $\alpha < 1$ and p_z is also less than one. Therefore, for a lead digital filter $\beta > 1$. For a lag digital filter $\beta < 1$. (Note that the condition on β is just the opposite for that on α.)

Because (11) and (14) have the same mathematical form, the z-plane compensator design procedures via the DIR techniques are essentially the same as those for designing a compensator for a continuous-time system.[3]

VI. Example of DIG Design: Guillaman-Truxal (G-T) Compensation Method

The figures of merit for the control system of Fig. 2 where

$$G_x(s) = \frac{0.4767}{s(s+1)}$$

and T = 0.1 sec are: $M_p = 1.043$, $t_p = 6.45$ sec, $t_s = 8.65$ sec, and $K_1 = 0.4765\ \text{sec}^{-1}$. The control ratio for the corresponding PCT system is

$$\frac{C(s)}{R(s)} = \frac{9.534}{(s+0.4875\pm j0.4883)(s+20.03)} \tag{19}$$

Consider the case where the figures of merit of the basic system are to be improved as follows: t_p and t_s are to be cut by one-half and some improvement in K_1 is desired while maintaining $M_p \leq 1.10$. Further, assume that the compensator model of Fig. 4(a) is constrained to increase the order of the system to four.

Based upon these specifications the following factors are used to derive the desired control ratio model:

(1) The real part $|\sigma_{1,2}|$ of the dominant roots is selected to be at least twice that of (19) based upon $T_s = 4/|\sigma_{1,2}|$, (2) the dominant roots are selected such that $\zeta = 0.7071$ in order to try to maintain $M_p \leq 1.10$, and (3) the s-plane pole-zero combination of $z_1 = -1.4$ and $p_3 = -1.1$ is added to minimize the increase in the overshoot which occurs when transforming from the continuous-time model to the sampled-data model. This selection of values is made in order to meet the desired performance specifications. Thus, the following continuous-time control ratio model is achieved.

$$\left.\frac{C(s)}{R(s)}\right|_M = \frac{15.714(s + 1.4)}{(s^2 + 2s + 2)(s + 1.1)(s + 10)} \tag{20}$$

Although the zero-pole combination, -1.4 and -1.1, of (20) lie just outside the allowable region of Fig. 1, this aspect is overlooked for a first trial design. Applying the Tustin transformation to (20), for T = 0.1, yields

$$\left.\frac{C(z)}{R(z)}\right|_{TU} = \frac{1.202 \times 10^{-3}(z + 1)^3(z - 0.8692)}{(z - 0.9005 \pm j0.0905)(z - 0.8957)(z - 0.3333)} = \frac{N(z)}{D(z)} \tag{21}$$

Applying the G-T method yields the following transfer function of the digital compensator of Fig. 4.

$$D_c(z) = \frac{N(z)}{[D(z) - N(z)]G_z(z)} = \frac{E_1(z)}{E_2(z)}$$

$$= \frac{0.5218(z + 1)^3(z - 0.9048)(z - 0.3692)}{(z - 0.8471 \pm j0.03753)(z - 0.3420)(z + 0.9672)} \tag{22}$$

Note, that as a consequence of the use of the G-T method and the Tustin approximation, the order of the numerator of $D_c(z)$ is greater than the order of the denominator by one.

A practical approach to achieving a physically realizable $D_c(z)$ is to replace one of the $(z + 1)$ factors which appear as a result of the Tustin transformation, by its d-c gain factor [2] of $(z + 1)|_{z=1} = 2$ in the numerator of $D_c(z)$ to yield

$$D_c(z) = \frac{K_{zc}(z + 1)^2(z - 0.9048)(z - 0.86921)}{(z - 0.8471 \pm j0.03753)(z - 0.3420)(z + 0.9672)} \qquad (23)$$

where $K_{zc} = 2(0.5218) = 1.0436$. With this controller, the control system's figures of merit are: $M_p = 1.031$, $t_p = 3.55$ sec, $t_s = 4.25$ sec, and $K_1 = 0.77198\ \text{sec}^{-1}$. The specific value of $t_p \leq 6.45/2$ can be met by increasing the value of K_{zc} to 1.14918.

As illustrated by this example a physically unrealizable controller may result when applying the Guillemin-Truxal method to $[C(z)/R(z)]_{TU}$. *In order to maintain the d-c gain and achieve a physically realizable controller, one approach, as applied to this example, is to replace one or more (z + 1) numerator factors of $D_c(z)$ by the d-c gain factor of 2.*

VII. Conclusions

By the use of the Padé approximation and the Tustin transformation, a sampled-data control system may be transformed into a PCT control system. As the examples illustrate, when the rules governing this transformation are satisfied the analysis and design of a PCT system model is a practical approach for the analysis and design of a sampled-data control system. The standard first-order z-plane compensator, $K_{zc}(z-z_z)/(z-z_z/\beta)$, corresponds to the standard first-order s-plane compensator, $K_{sc}(s-z_s)/(s-z_s/\alpha)$, where for a lead compensator

$\beta < 1$ and $\alpha > 1$. A consequence of applying the Tustin transformation to $C(s)/R(s)$ of the PCT system and then applying the G-T method to $[C(z)/R(z)]_{TU}$ is that an unrealizable cascade digital compensator $D_c(z)$ results. This paper illustrates a method by which this $D_c(z)$ may be made realizable by replacing one or more $(z+1)$ factor in the numerator, due to the Tustin transformation, by its d-c gain factor of two.

References

1. Oppenheim, A. V. and R. W. Schafer "Digital Signal Processing," Prentice-Hall, Englewood Cliffs, NJ, 19

2. Houpis, C. H. and G. B. Lamont "Digital Control System (Theory, Hardware, Software)," McGraw-Hill Book Co., NY, NY, Fall, 1983.

3. D'Azzo, J. J. and C. H. Houpis "Linear Control Systems Analysis and Design: Conventional and Modern," McGraw-Hill Book Co., NY, NY, 2nd Ed, 1981.

4. Wall, H. S. "Analytic Theory of Continued Fractions," D. Van Nostrand Company, Inc., 1948.

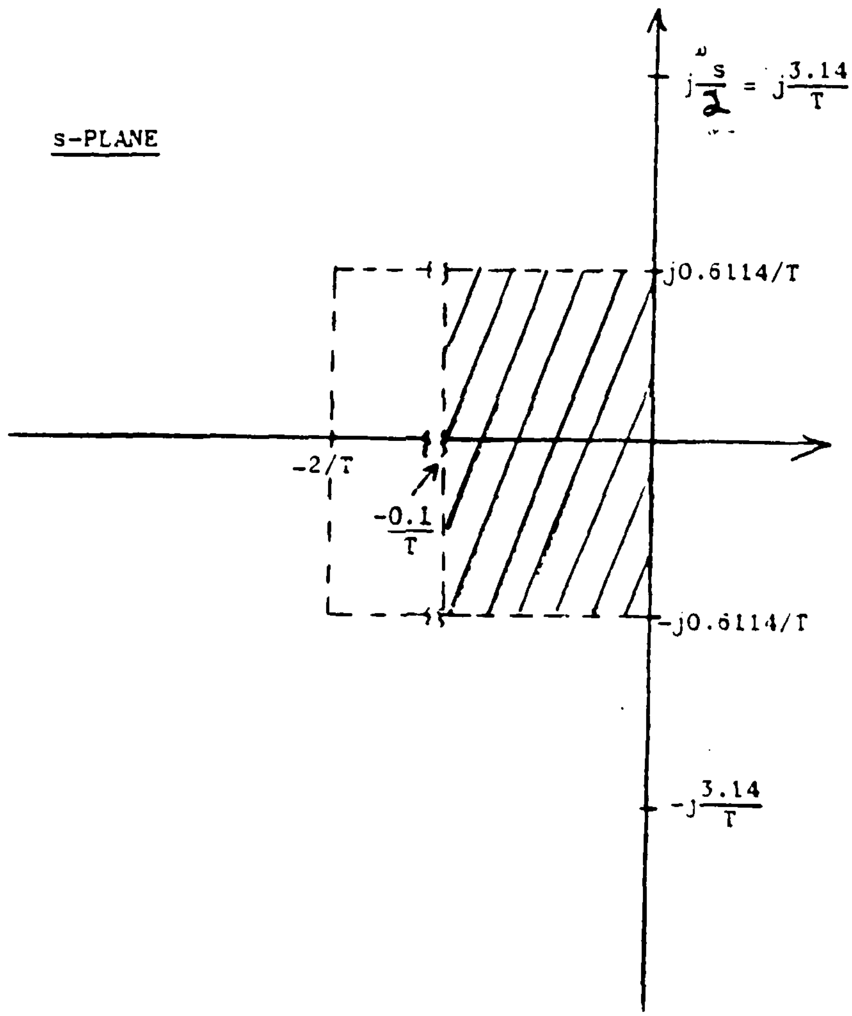

Fig. 1. Allowable location (shaded area) of dominant poles and zeros in s-plane for a good Tustin approximation.

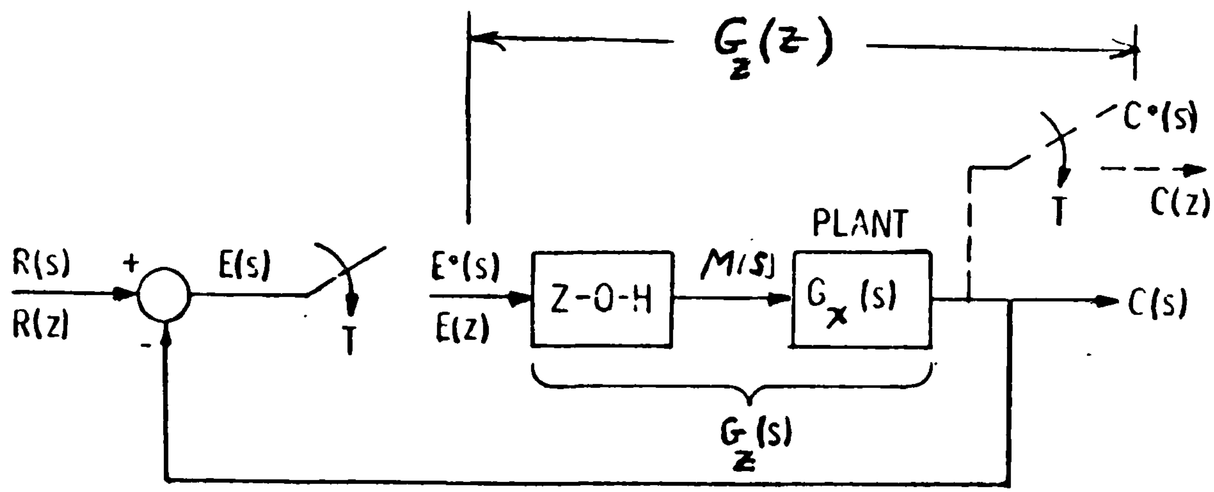

Fig. 2. The uncompensated sampled-data control system.

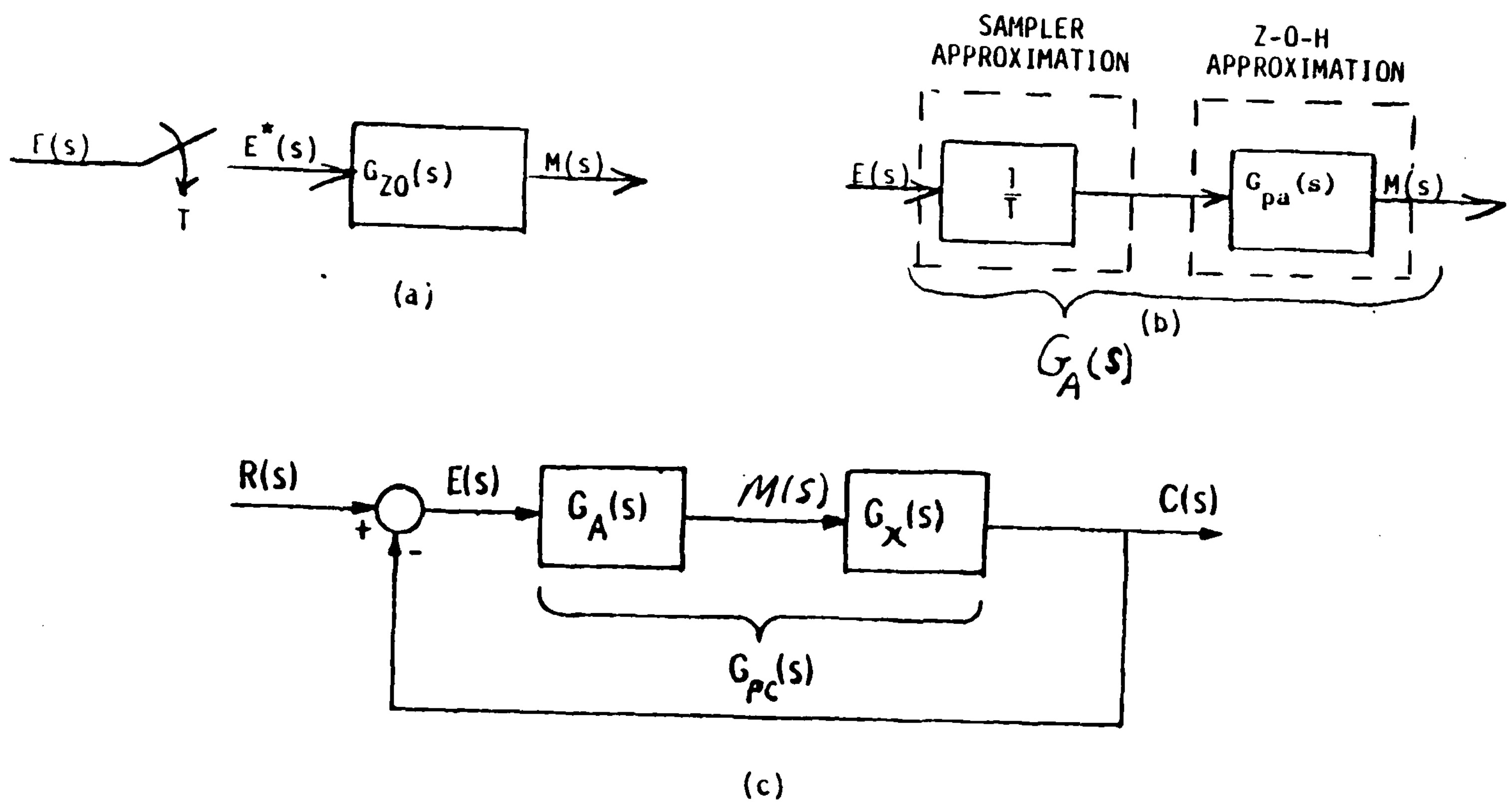

Fig. 3. (a) Sampler and Z-O-H; (b) Approximations of the Sampler and Z-O-H; and the Approximate Continuous-Time Control System Equivalent of Fig. 7-8.

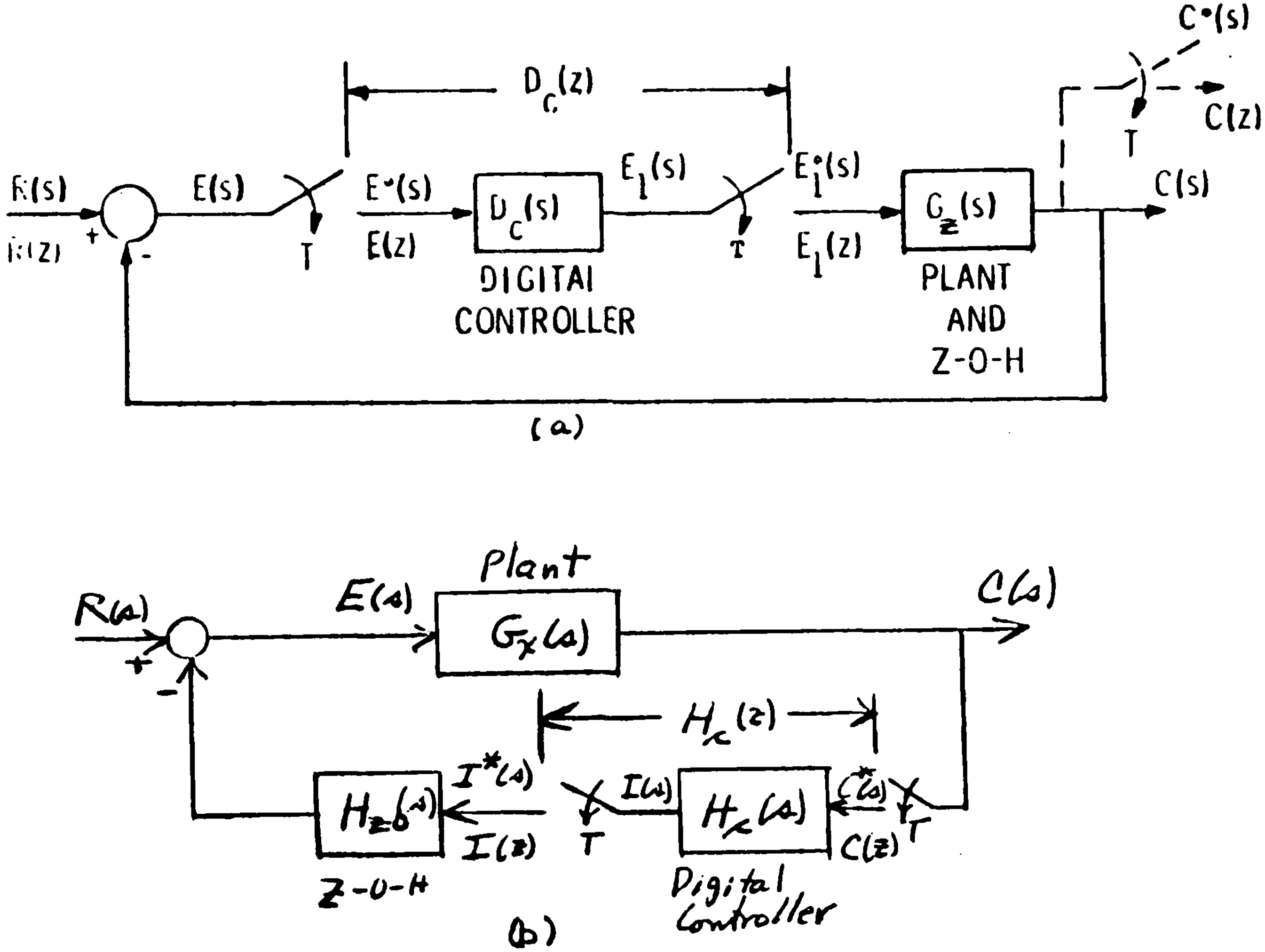

Fig. 4. A compensated sampled-data or a digital control system:

(a) cascade and (b) feedback compensation.

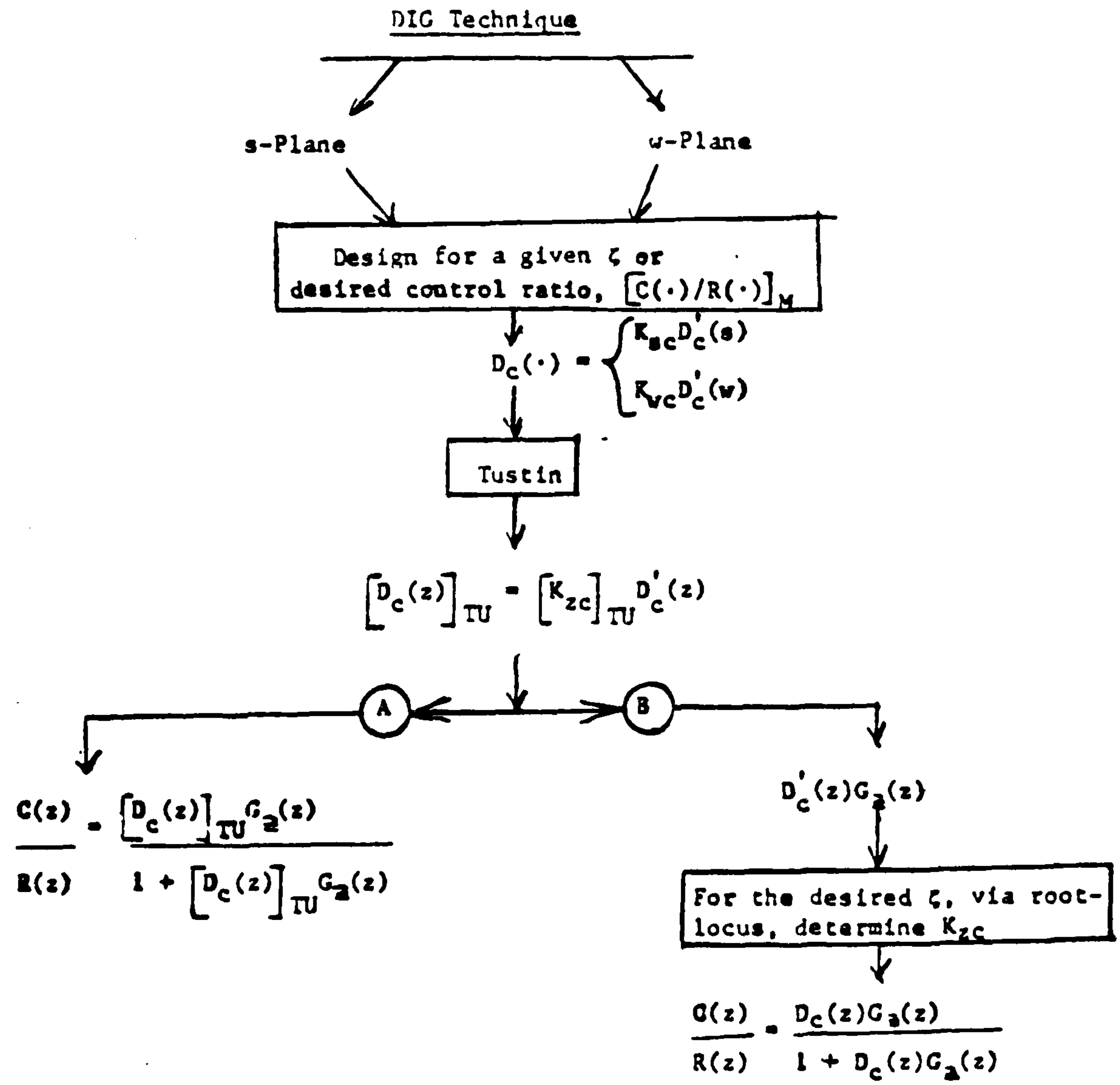

Fig. 5. DIG design philosophy for Fig. 11-1(a).

ASYMPTOTIC NON-NULL DISTRIBUTION OF A TEST OF EQUALITY OF EXPONENTIAL POPULATIONS

R. W. Kulp and B. N. Nagarsenker

Air Force Institute of Technology

Wright-Patterson Air Force Base, Ohio

Key Words and Phrases: exponential populations; likelihood ratio criterion; asymptotic non-null distribution; Chi-square distributions.

Abstract

In this paper asymptotic expansions of the non-null distribution of the likelihood ratio criterion for testing the equality of several one parameter exponential distributions are obtained under local alternatives. These expansions are in terms of Chi-square distributions.

1. Introduction

Suppose that p samples are available and that the ith sample contains n observations x_{ij} with mean $\bar{x}_i$ ($i = 1,2,\ldots,p$; $j = 1,2,\ldots,n$) and has been drawn from an exponential distribution with probability density given by

$$\begin{aligned} f(x) &= \sigma_i^{-1} \exp(-x/\sigma_i) && x > 0,\ \sigma_i > 0 \\ &= 0 && \text{otherwise } (i=1,2,\ldots,p) \end{aligned} \tag{1.1}$$

A test of hypothesis H_0 that the p samples have been randomly drawn from the same population is equivalent to testing that the p exponential distributions in (1.1) are identical. In other words, it is desired to test the hypothesis

$$H_0: \sigma_1 = \sigma_2 = \ldots = \sigma_p$$

against the general alternatives. The likelihood ratio criterion for testing H_0 is given by

$$\lambda = L^n = \left[\prod_{i=1}^{p} (\bar{x}_i/\bar{x}) \right]^n \tag{1.2}$$

where $\bar{x}$ is the mean of the combined sample. The null distribution of L has been considered by Jain, Rathie and Shah (1975), Nagarsenker (1980), Nagarsenker et al. (1982) while the non-null distribution has been discussed by Mathai (1979). For further references see Johnson and Kotz (1970).

In this paper, we first obtain the non-null moments in terms of zonal polynomials and then use these to obtain the asymptotic expansion of the distribution of $-2(n-u) \ln L$ where $u = (p+1)/6p$ (see Nagarsenker (1980)), under the sequence of local alternatives (see Khatri and Srivastava (1974))

$$\text{(i)} \quad \underset{\sim}{I} - q\underset{\sim}{\Sigma}^{-1} = \underset{\sim}{P}/m \quad \text{and} \quad \text{(ii)} \quad \underset{\sim}{I} - q^{-1}\underset{\sim}{\Sigma} = \underset{\sim}{Q}/m \tag{1.3}$$

where $\underset{\sim}{\Sigma} = \mathrm{diag}\,(\sigma_1,\sigma_2,\ldots,\sigma_p)$, $m = n - u$, $0 < q < \infty$ while $\underset{\sim}{P}$ and $\underset{\sim}{Q}$ are fixed matrices as m tends to infinity.

2. Preliminaries

We need the following lemmas in the sequel.

Lemma 1. The non-null hth moment of λ defined in (1.2) is given by

$$E(\lambda^h) = \left[p^{nh} \frac{\Gamma(nh+n)}{\Gamma(n)} \right]^p |q\underset{\sim}{\Sigma}^{-1}|^n \sum_{k=0}^{\infty} \sum_{\kappa} \frac{(nh+n)_\kappa \Gamma(pn+k)}{k!\,\Gamma(pnh+pn+k)} C_\kappa(\underset{\sim}{M}) \tag{2.1}$$

where $\underset{\sim}{M} = \underset{\sim}{I} - q\underset{\sim}{\Sigma}^{-1}$, $0 < q < \infty$ and $\underset{\sim}{\Sigma} = \mathrm{diag}\,(\sigma_1,\sigma_2,\ldots,\sigma_p)$.

Proof. To obtain the hth moment of λ, we shall essentially use the method given in Wilks (1946) and the fact that $\bar{x}_i$ are independently distributed as gammas with parameters n and σ_i/n, $i = 1,2,\ldots,p$. For this consider the function $\phi(\theta)$ where

$$\phi(\theta) = E\left[\left|\prod_{i=1}^{p}(\bar{x}_i)^{nh}\right| e^{\theta\bar{x}}\right].$$

It can be easily shown that

$$\phi(\theta) = \left[\frac{\Gamma(nh+n)}{\Gamma(n)}\right]^p |\Sigma/n|^{nh} |I-\theta_1\Sigma|^{-(nh+n)} \qquad (2.2)$$

where $\theta_1 = \theta/np$. Using the following identity (see Khatri and Srivastava (1971)),

$$|I-\theta_1\Sigma|^{-(n+nh)} = (1-\theta_1 q)^{-p(nh+n)} |q^{-1}\Sigma|^{-(nh+n)} \sum_{k=0}^{\infty}\sum_{\kappa} \frac{(nh+n)_\kappa C_\kappa(M)}{(1-\theta_1 q)^k\, k!}$$

where $0 < q < \infty$ and can be chosen such that the expansion in the series form is valid, i.e., θ_1 and q are such that

$$|1-q(ch_{max}\Sigma)^{-1}| < (1-q\theta_1).$$

$E(\lambda^h)$ is then obtained by evaluating $\frac{d^r\phi(\theta)}{d\theta^r}$ at $\theta = 0$ and then putting $r = -nh$ (see Wilks (1946) for the validity of such operation). This gives (2.1).

<u>Remark</u>. Taking $q = \sigma^2$, we get the null moments of λ given in Nagarsenker (1980).

<u>Lemma 2</u>. Let $C_\kappa(Z)$ be a zonal polynomial corresponding to the partition $\kappa = \{k_1,k_2,\ldots,k_p\}$ with $k_1 + k_2 + \ldots + k_p = k$ and $k_1 \geq k_2 \geq \ldots \geq k_p \geq 0$. Let

$$a_1(\kappa) = \sum_{i=1}^{p} k_i(k_i-i),\quad a_2(\kappa) = \sum_{i=1}^{p} k_i(4k_i^2-6ik_i+3i^2).$$

and $\sigma_r = tr(Z^r)$. Then the following equalities hold:

$$(1)\quad \sum_{k=0}^{\infty} \sum_{\kappa} \frac{C_{\kappa}(Z)}{(k-r)!} = \sigma_1^{r} e^{\sigma_1}$$

$$(2)\quad \sum_{k=0}^{\infty} \sum_{\kappa} \frac{a_1(\kappa)C_{\kappa}(Z)}{k!} = \sigma_2 e^{\sigma_1}$$

$$(3)\quad \sum_{k=1}^{\infty} \sum_{\kappa} \frac{a_1(\kappa)C_{\kappa}(Z)}{(k-1)!} = (2\sigma_2+\sigma_1\sigma_2)e^{\sigma_1}$$

$$(4)\quad \sum_{k=0} \sum_{\kappa} \frac{(a_1(\kappa))^2 C_{\kappa}(Z)}{k!} = (\sigma_1^2+\sigma_2+4\sigma_3+\sigma_2^2)e^{\sigma_1}$$

$$(5)\quad \sum_{k=0}^{\infty} \sum_{\kappa} \frac{a_2(\kappa)C_{\kappa}(Z)}{k!} = (4\sigma_3+3\sigma_2+3\sigma_1^2+\sigma_1)e^{\sigma_1}$$

$$(6)\quad \sum_{k=0}^{\infty} \sum_{\kappa} \frac{k^2 a_1(\kappa)C_{\kappa}(Z)}{k!} = (\sigma_1^2+5\sigma_1+4)\sigma_2 e^{\sigma_1}$$

(see Pillai and Nagarsenker (1972)).

Lemma 3. With the notation of lemma 1, for large m we have

$$(mg+a)_{\kappa} = (mg)^k \Big[1 + \frac{1}{mg} \{ka + \tfrac{1}{2} a_1(\kappa)\} + \frac{1}{24(mg)^2} \{12a^2 k(k-1)$$

$$+ 12a(k-1)a_1(\kappa) + 3a_1^2(\kappa) - a_2(\kappa) + k\} + O(m^{-3}) \Big]$$

(see Pillai and Nagarsenker (1972)).

3. Asymptotic Non-Null Distribution of L

In this section we shall obtain the asymptotic expansion of the distribution of $-2m \ln L$ in terms of $m = n - u$ increasing where $u = (p+1)/6p$ (see Nagarsenker (1980)), for the sequence of alternatives stated in (1.3).

Case 1. $(\underset{\sim}{I}-q\underset{\sim}{\Sigma}^{-1}) = \underset{\sim}{P}/m$.

Let $U = -2m \ln L$. Then from (2.1) the characteristic function $\psi(t)$ of U under this sequence of alternatives is given by

$$\psi(t) = \left[p^{-2mit} \frac{\Gamma(mg+u)}{\Gamma(m+u)} \right]^p |\underset{\sim}{I}-\underset{\sim}{P}/m|^{(m+u)} \sum_{k=0}^{\infty} \sum_{\kappa} \frac{T(\kappa)C_\kappa(\underset{\sim}{P}/m)}{k!} \tag{3.1}$$

where $g = (1-2it)$ and $T(\kappa) = \dfrac{(mg+u)_\kappa \Gamma(pm+pu+k)}{\Gamma(pmg+pu+k)}$.

Now using the expansion

$$\ln|\underset{\sim}{I}-\underset{\sim}{P}/m| = -\sigma_1/m - \sigma_2/2m^2 - \sigma_3/3m^3 + \underset{\sim}{O}(m^{-4})$$

where $\sigma_i = \mathrm{tr}(\underset{\sim}{P}^i)$, we have

$$|\underset{\sim}{I}-\underset{\sim}{P}/m|^{(m+u)} = e^{-\sigma_1}\left[1 + \frac{C_1}{m} + \frac{C_2}{m^2} + \underset{\sim}{O}(m^{-3})\right] \tag{3.2}$$

where $C_1 = -\dfrac{\sigma_2}{2} - u\sigma_1$ and $C_2 = -\left(\dfrac{\sigma_3}{3} + \dfrac{u\sigma_2}{2}\right) + C_1^2/2$.

Again using Stirling's asymptotic formula for the logarithm of a gamma function and then using lemmas 1-3 and (3.2) in (3.1), we have up to $\underset{\sim}{O}(m^{-3})$,

$$\psi(t) = g^{-v}\left[1 + \frac{b_1}{2pm}(1-g^{-1}) + \frac{1}{(2pm)^2}\sum_{i=0}^{2} \beta_i g^i + O(m^{-3})\right] \tag{3.3}$$

where $v = \dfrac{p-1}{2}$, $b_1 = \sigma_1^2 - p\sigma_2$, $b_2 = \sigma_1^3 - p^2\sigma_3$;

$$\beta_0 = \frac{1}{2}b_1^2 + \frac{4}{3}b_2 + 2upb_1 + (p+1)^2(p-1)/36$$

$$\beta_1 = -b_1^2 - 4\sigma_1 b_1 - 2b_1 - 4upb_1$$

and $\beta_2 = -(\beta_0+\beta_1)$.

Inverting the characteristic function $\phi(t)$ in (3.3), we have the following theorem.

<u>Theorem 3.1</u>. Under the sequence of alternatives $\underset{\sim}{I}-q\underset{\sim}{\Sigma}^{-1} = \underset{\sim}{P}/m$, the non-null distribution of $-2m \ln L$ where L is given in (1.2) can be expanded asymptotically for large $m = n - u$, $u = (p+1)/6p$ as follows:

$$P(-2m \ln L \le x) = P(\chi^2_f \le x) + \frac{b_1}{2pm} [P(\chi^2_f \le x) - P(\chi^2_{f+2} \le x)]$$

$$+ \frac{1}{(2pm)^2} \left[\sum_{i=0}^{2} \beta_i P(\chi^2_{f+2i} \le x) \right] + \underset{\sim}{O}(m^{-3})$$

where $f = 2v = p - 1$, χ^2_f is the chi-square variable with f degrees of freedom and the coefficients b_1, β_0, β_1 and β_2 are given in (3.3).

<u>Case 2</u>. $(\underset{\sim}{I}-q^{-1}\underset{\sim}{\Sigma}) = \underset{\sim}{Q}/m$.

We have $\underset{\sim}{I}-q\underset{\sim}{\Sigma}^{-1} = -\underset{\sim}{Q}(\underset{\sim}{I}-\underset{\sim}{Q}/m)^{-1}/m$. So proceeding as in the case 1 by replacing $\underset{\sim}{P}$ by $-\underset{\sim}{Q}(\underset{\sim}{I}-\underset{\sim}{Q}/m)^{-1}$ and retaining terms of the order of m^{-2} we have the following theorem.

<u>Theorem 3.2</u>. Under the sequence of alternatives $\underset{\sim}{I} - q^{-1}\underset{\sim}{\Sigma} = \underset{\sim}{Q}/m$, the non-null distribution of $-2m \ln L$ can be expanded asymptotically for large m as follows:

$$P(-2m \ln L \le x) = P(\chi^2_f \le x) + \frac{a_1}{2pm} [P(\chi^2_f \le x) - P(\chi^2_{f+2} \le x)]$$

$$+ \frac{1}{(2pm)^2} \left[\sum_{i=0}^{2} \alpha_i P(\chi^2_{f+2i} \le x) \right] + O(m^{-3})$$

where $a_1 = (\text{tr } \underset{\sim}{Q})^2 - p \text{ tr } Q^2$,

$a_2 = (\text{tr } \underset{\sim}{Q})^3 - p^2 \text{ tr } Q^3$,

$$\alpha_0 = \frac{(p+1)^2(p-1)}{36} + \frac{1}{2}a_1^2 - 4(\mathrm{tr}\ \underset{\sim}{Q})a_1 + 2upa_1 + 8a_2/3$$

$$\alpha_1 = -a_1^2 + 2a_1 + 8(\mathrm{tr}\ \underset{\sim}{Q})a_1 - 4upa_1 + 4a_2$$

and $\alpha_2 = -(\alpha_0+\alpha_1)$.

Remark. It may be noted that when $\underset{\sim}{P} = \underset{\sim}{Q} = \underset{\sim}{0}$, the asymptotic expansion in the two cases reduces to that of Box's approximation given in (4.2) of Nagarsenker (1980) for the null hypothesis H_0.

Bibliography

Jain, S. K., Rathie, P. N. and Shah, M. C. (1975). The exact distributions of certain likelihood ratio criteria. Sankhya, Ser. A, 37, pp. 150-163.

Johnson, N. L. and Kotz, S. (1970). Distributions in Statistics: Continuous Distributions I. Boston: Houghton Mifflin Company.

Khatri, C. G. and Srivastava, M. S. (1971). On exact non-null distributions of likelihood ratio criteria for sphericity test and equality of two covariance matrices. Sankhya, Ser. A, 33, 201-206.

Khatri, C. G. and Srivastava, M. S. (1974). Asymptotic expansions of the non-null distributions of likelihood ratio criteria for covariance matrices. Ann. Statist., 2, 109-117.

Mathai, A. M. (1979). On the non-null distributions of test statistics connected with exponential populations. Comm. Statist., A8, 47-55.

Nagarsenker, P. B. (1980). On a test of equality of several exponential survival distributions. Biometrika, 67, 475-478.

Nagarsenker, B. N., McCulloch, J. A. Loch, C. A. and Nagarsenker, P. B. (1982). On the distribution of LRT for testing the equality of exponential distributions. Comm. Statist. - Theor. Meth.,A11, 1119-1127.

Pillai, K. C. S. and Nagarsenker, B. N. (1972). On the distributions of a class of statistics in multivariate analysis. J. Multivariate Anal., 2, 96-114.

Wilks, S. S. (1946). Sample criteria for testing equality of means, equality of variances and equality of covariances in a normal multivariate distribution. Ann. Math. Statist., 17, 257-281.

Irrotational and Solenoidal Waves
in General Coordinates

by

D. A. Lee
Air Force Institute of Technology

Abstract

Tensor analysis and some identities are applied to make tolerably convenient forms of equations for irrotational and solenoidal components of elastodynamic displacement fields, valid in arbitrary admissible curvilinear coordinates.

Introduction

Displacement fields of elastodynamic waves, i.e. suitably smooth vector functions $\boldsymbol{u}(\boldsymbol{x},t)$ which are solutions of the Navier-Cauchy equations

$$a^2\nabla(\nabla\cdot\boldsymbol{u})-b^2\nabla\times\nabla\times\boldsymbol{u}=\frac{\partial^2\boldsymbol{u}}{\partial t^2} \tag{1}$$

can always be written as sums of irrotational and solenoidal vector functions, in the form

$$\boldsymbol{u}=\nabla\varphi(y,z,t)+\nabla\times\boldsymbol{A} \tag{2}$$

where the vector function $\boldsymbol{A}(\boldsymbol{x},t)$ is solenoidal, i.e.

$$\nabla\cdot\boldsymbol{A}\equiv 0 \tag{3}$$

(Reference [1]). The scalar φ satisfies the scalar wave equation

$$a^2\nabla^2\varphi=\frac{\partial^2\varphi}{\partial t^2} \tag{4}$$

and the vector $\boldsymbol{A}$ satisfies the vector wave equation

$$b^2\nabla^2\boldsymbol{A}=\frac{\partial^2\boldsymbol{A}}{\partial t^2} \tag{5}$$

In (5),

$$\begin{aligned}\nabla^2\boldsymbol{A}&\equiv\nabla(\nabla\cdot\boldsymbol{A})-\nabla\times\nabla\times\boldsymbol{A}\\&=-\nabla\times\nabla\times\boldsymbol{A}\end{aligned}$$

in view of (3) (Reference [2]).

Often it is more convenient to find the scalar φ and the vector $\mathbf{A}$ representing an elastodynamic displacement field, than it is to find directly the field itself. Often, too, one wishes to work in a coordinate system convenient for the problem at hand, and then, particularly for non-orthogonal curvilinear coordinates, a blunt evaluation of the spatial differential operators in (4) and (5) may be very unwieldy. This paper presents a development of the representation (2) valid for arbitrary curvilinear coordinates, together with convenient means for writing out generalizations of (4) and (5). In particular, the generalized equations can be written out explicitly without evaluating Christoffel symbols.

Irrotational and Solenoidal waves in General Coordinates

In general coordinates, an irrotational wave's displacement field can be written

$$u^i = g^{ik}\varphi_{,k} \tag{9}$$

while a solenoidal wave's displacement field can be expressed in the form

$$u^i = \frac{1}{\sqrt{g}}\varepsilon^{ijk} A_{k,j} \tag{10}$$

where the once-covariant tensor A_k is a function of position and time, as is the scalar φ.

In (9) and (10), g^{ij} denotes the contravariant metric tensor elements of the coordinate system. A comma preceeding an index denotes covariant differentiation, e.g.

$$A_{k,j} \equiv \frac{\partial A_k}{\partial x^j} - \begin{Bmatrix} m \\ kj \end{Bmatrix} A_m$$

The permutation tensor elements ε^{ijk} may be defined as

$$\varepsilon^{ijk} \equiv \begin{Bmatrix} sgn(\pi) \text{ if } (i,j,k) \text{ is a permutation } \pi \text{ of } (1,2,3) \\ 0, \text{ otherwise} \end{Bmatrix} = \varepsilon_{ijk}$$

These elements are special in that they transform both as three-times contravariant relative tensor elements of weight $+1$ and as three-times covariant relative tensor elements of weight -1.

The Navier-Cauchy equations (4) may be written in general coordinates as

$$a^2 u^k{}_{,km} g^{mi} - b^2 \varepsilon^{ijk}\varepsilon_{krm} u^m{}_{,pj} g^{pr} = \frac{\partial^2 u^i}{\partial t^2} \tag{11}$$

Seeking an irrotational solution of (11), one finds that

$$u^m{}_{,p} g^{pk} = g^{mr}\varphi_{,rp} g^{pk}$$

is symmetric in m and k, so that the second term of the left side of (11) is identically zero. The remaining terms of (11) require

$$\left[a^2 g^{rj}\varphi_{,rj}-\frac{\partial^2\varphi}{\partial t^2}\right]_{,k} g^{ik}=0$$

which will surely be met if

$$a^2 g^{mj}\varphi_{,mj} = \frac{\partial^2\varphi}{\partial t^2} \tag{12}$$

One may take (12) as the defining equation for irrotational waves.

Turning to solenoidal waves with displacement fields of the form (10), one sees that

$$u^m{}_{,m}=\frac{1}{\sqrt{g}}\varepsilon^{mjk}A_{k,jm}\equiv 0$$

by the symmetry of $A_{k,jm}$ with respect to j and m, so that now the first term on the left side of (11) is identically zero. The remaining terms lead, after some manipulation, to

$$\varepsilon^{ijk}\left[-b^2\varepsilon_{knm}\varepsilon^{mrs}g^{pn}A_{s,rp}-\frac{\partial^2 A_k}{\partial t^2}\right]_{,j}=0 \tag{13}$$

for which it is sufficient that the quantity in square brackets is identically zero. But that condition leads, after use of the identity

$$\varepsilon_{knm}\varepsilon^{mrs}\equiv\delta_k^r\delta_n^s-\delta_k^s\delta_n^r$$

to

$$b^2\left[g^{pr}A_{k,rp}-g^{sp}A_{s,pk}\right]=\frac{\partial^2 A_k}{\partial t^2}$$

But the defining tensor A_k of the solenoidal waves is itself solenoidal, so that

$$g^{sp}A_{s,p}\equiv 0 \tag{14}$$

Then the defining equations for a solenoidal wave may be written as (14), together with

$$b^2 g^{pr}A_{k,rp}=\frac{\partial^2 A_k}{\partial t^2} \tag{15}$$

One could, of course, have written (12), (14) and (15) as tensorially consistent generalizations of (4),(3), and (5), respectively. It is well, however, to carry through a complete treatment, starting with explicit definitions (9) and (10), to be certain the work is self-consistent.

Moreover, while the forms of tensor equations (12) and (15) are succinct and easy to remember, these forms aren't usually the most convenient ones to use for writing out the detailed statements which those equations imply in a given coordinate system. Direct evaluation of (15), for example, usually requires evaluation of Christoffel symbols and derivatives of Christoffel symbols.

Explicit "unfolding" of (12) for a specific coordinate system is made easier by the well-known identity [3]

$$g^{rm} \varphi_{,rm} \equiv \frac{1}{\sqrt{g}} \frac{\partial}{\partial x^n} \left[\sqrt{g} \frac{\partial \varphi}{\partial x^n} \right] \tag{16}$$

by virtue of which (12) is equivalent to

$$\frac{a^2}{\sqrt{g}} \frac{\partial}{\partial x^n} \left[\sqrt{g} \frac{\partial \varphi}{\partial x^n} \right] = \frac{\partial^2 \varphi}{\partial t^2} \tag{17}$$

Explicit writing-out of (15) is probably simplified in most cases by the following considerations: The elements T^i, defined by

$$T^i \equiv \frac{1}{\sqrt{g}} \varepsilon^{ijk} A_{k,j}$$

are once-contravariant (oriented) tensor coordinates. Also, they may be evaluated explicitly without evaluating Christoffel symbols, since

$$\varepsilon^{ijk} A_{k,j} \equiv \varepsilon^{ijk} \frac{\partial A_k}{\partial x^j} - \varepsilon^{ijk} \begin{Bmatrix} n \\ jk \end{Bmatrix} A_n \tag{18}$$

and the last term in (18) is identically zero by virtue of the symmetry of the Christoffel symbol in its lower indices j and k, and the anti-symmetry of ε^{ijk} in those indices. Thus the S_i,

$$S_i \equiv g_{ir} T^r = \frac{g_{ir}}{\sqrt{g}} \varepsilon^{rjk} \frac{\partial A_k}{\partial x^j}$$

are once covariant, oriented tensor coordinates. Repeating the previous arguments of this paragraph then shows that the R_i,

$$R_i \equiv \frac{g_{im}}{\sqrt{g}} \varepsilon^{mnp} S_{p,n}$$

$$= \frac{g_{im}}{\sqrt{g}} \varepsilon^{mnp} \frac{\partial S_p}{\partial x^n} = \frac{g_{im}}{\sqrt{g}} \varepsilon^{mnp} \frac{\partial}{\partial x^n} \left[\frac{g_{pr}}{\sqrt{g}} \varepsilon^{rjk} \frac{\partial A_k}{\partial x^j} \right]$$

are once covariant tensor coordinates, which can be written out without evaluating Christoffel symbols. In rectangular Cartesian coordinates,

$$R_k = \varepsilon_{knp} \, \varepsilon_{pjr} \frac{\partial^2 A_r}{\partial x^j \partial x^n}$$

Now, the quantity

$$V_k \equiv \varepsilon_{knm} \, \varepsilon^{mrs} A_{s,rp}$$

appearing in (13) is also a set of once covariant tensor coordinates. In rectangular cartesian coordinates,

$$V_k = \varepsilon_{knm} \, \varepsilon_{mrs} \frac{\partial^2 A_s}{\partial x^r \partial x^n} = R_k$$

But then $R_k = V_k$, since coordinates of a given tensor character which are equal in one coordinate system are equal in all coordinate systems.

Thus a set of equations equivalent to (14), (15) is (14) and

$$-b^2 \frac{g_{im}}{\sqrt{g}} \varepsilon^{mnp} \frac{\partial}{\partial x^n} \left[\frac{g_{pr}}{\sqrt{g}} \varepsilon^{rjk} \frac{\partial A_k}{\partial x^j} \right] = \frac{\partial^2 A_i}{\partial t^2} \tag{19}$$

Equation (19) is likely to be more convenient for writing out than equation (15), since no Christoffel symbols appear in (19). Moreover, the operations on the left side of (19) can all be accomplished by fairly straightforward matrix multiplications and differentiations.

References

1. Sternberg, E., Arch. Rat. Mech. Anal. 6 , 34 (1960)

2. Achenbach, J. D., *Wave Propagation in Elastic Solids* , Section 3.4, pages 85 ff , American Elsevier, New York, 1973

3. Sokolnikoff, I. S. , *Tensor Analysis* , page 89, Wiley, New York, 1964

SOME PROBLEMS OF ESTIMATION WHEN SOME PRIOR INFORMATION IS AVAILABLE

Albert H. Moore
Air Force Institute of Technology
Wright-Patterson Air Force Base

Abstract

In this paper we will consider problems where, without prior information, the classical best unbiased estimators are known to be admissible. If we assume enough prior information is available to bound the parameter, but not enough to specify a prior density we will show that the classical U.M.V.U. estimators are inadmissible by exhibiting alternative biased estimators with uniformly smaller mean square error. This is possible because if we examine the mean square error we see that the uniformly minimum variance unbiased (U.M.V.U.) estimators are best only at the boundary points in the parameter space. If enough prior information exists to exclude these boundary points then the classical estimator should be inadmissible. With this insight we are able to show that the classical U.M.V.U. estimators are inadmissible in a new way.

In Sections 2-6, we give several examples where the U.M.V.U. estimator is inadmissible when enough prior information is available to bound θ. Throughout this paper we use squared error loss function.

1. Introduction

Let x be a random variable taking values in a measure space ($\mathfrak{X}$, B, μ). In standard statistical problems $\mathfrak{X}$ is an n-dimensional Euclidean space E_n and B is a Borel σ-field and μ is either a counting measure or Lebesgue measure. It is also assumed that x has a density $f(x,\theta), \theta \varepsilon \Omega$ = parameter space, with respect to the appropriate measure.

In estimation problems, we assume f is known but θ is unknown. We observe X = x, and want to find a measureable function of X = x, and use it to estimate θ. The classical approaches are maximum likelihood estimation (M.L.E.) and U.M.V.U. estimation. In the decision theory approach Bayes and minimax estimators are generally used.

In U.M.V.U. estimation any prior information is disregarded while on the other hand in many instances the Bayes approach requires too much prior information. In many cases we have only partial information.

Robbins [5] proposed an empirical Bayes approach which makes use of past data to obtain an empirical estimate of the prior density of the parameter for Bayes estimation. Katz [3] investigated some properties of point estimators when an upper or lower bound for the parameters is given in advance. He considered the square error loss function and derived admissible minimax estimators using Bayesian approach with a suitable prior. Lehmann [4] showed that for N(θ,1) with $a \le \theta \le b$, $\bar{x}$ is not admissible and not minimax. In addition he showed that if $\theta \geq a$, then $\bar{x}$ is minimax but not admissible. Skibinsky and Cote [6] showed that with certain prior information about the distribution of θ for the binomial $\bar{x}$ is inadmissible, and in a similar fashion he showed that $\bar{x}$ is an inadmissible estimator for the mean of the normal density. Kale [2] showed that for truncated parameter spaces the M.L.E. is inadmissible by showing it is not a proper Bayes estimator for the exponential family of densities with continuous parameter space. Blum and Rosenblatt [1] discussed Bayes estimation where it was assumed that the family of distributions which the prior came from is known.

2. The Binomial Distribution. Let X be an observation from a binomial distribution with density $b(x,n,\theta) = \binom{n}{x} \theta^x(1-\theta)^{n-x}$, $0 \leq \theta \leq 1$. The statistic X is a complete sufficient statistic for θ. The best unbiased estimator $\hat{\theta}_1$ of θ is x/n. The risk of $\hat{\theta}_1$ is given by

$$R_{\hat{\theta}_1}(\theta) = \frac{(1-\theta)(\theta)}{n} . \qquad (1)$$

Consider an estimator $\hat{\theta}_2$ of the form $\hat{\theta}_2 = k\hat{\theta}_1$. The value of k which minimizes the mean square error is easily seen to be

$$k = \frac{\theta^2}{\frac{\theta(1-\theta)}{n} + \theta^2} = \frac{\theta}{\frac{1-\theta}{n} + \theta} . \qquad (2)$$

Here the best estimator of the form $k\hat{\theta}_1$ is a function of the unknown parameter θ. However we can say that

$$\hat{\theta}_3 = \frac{\ell}{\frac{1-\ell}{n} + \ell}\,\hat{\theta}_1, 0 \le \ell \le 1 \tag{3}$$

is the best estimator for θ of the form $k\hat{\theta}_1$ at the parameter value $\theta = \ell$. It is interesting to see that the U.M.V.U. estimator is best (in the mean square sense) only at the parameter value $\theta = 1$. The estimators $\hat{\theta}_3$ are an infinite family of admissible estimators. Suppose we have prior information that $\theta \le \ell < 1$.

__Theorem 1__. If it is known that $\theta \le \ell < 1$ then $\hat{\theta}_3 = \dfrac{\ell\hat{\theta}_1}{\frac{1-\ell}{n} + \ell}$ is an estimator with uniformly smaller mean square error than $\hat{\theta}_1$ and hence $\hat{\theta}_1$ is inadmissible.

__Proof__. Consider $\hat{\theta}_3 = k\hat{\theta}_1$ where $k = \dfrac{n\ell}{(1-\ell) + n\ell}$.

$$\text{m.s.e. of } \hat{\theta}_3 = \frac{\theta(1-\theta)}{n} \; \frac{n^2\ell^2(1-\theta)-2n\ell\theta+n\ell^2\theta+n\theta}{(1-\theta)[1-2\ell+2n\ell-2n\ell^2+\ell^2-n^2\ell^2]}$$

$$= \frac{\theta(1-\theta)}{n} \; \frac{n\theta[1-2\ell+\ell^2]+n^2\ell^2(1-\theta)}{(1-\theta)[1-2\ell+\ell^2]+2n\ell(1-\theta)+n^2\ell^2(1-\theta)}$$

$$= \frac{\theta(1-\theta)}{n} \; \frac{n\theta + \dfrac{n^2\ell^2(1-\theta)}{1-2\ell+\ell^2}}{(1-\theta)\left[1 + \dfrac{2n\ell(1-\ell)}{(1-\ell)^2}\right] + \dfrac{n^2\ell^2(1-\theta)}{1-2\ell+\ell^2}}$$

$$\theta = \frac{\theta(1-\theta)}{n} \quad \frac{n\theta + n^2\ell^2(1-\theta)/1-2\ell+\ell^2}{\frac{2n\ell(1-\theta)}{(1-\ell)} + (1-\theta) + n^2\ell^2(1-\theta)/1-2\ell+\ell^2} .$$

Since $\theta \le \ell$ the fraction $\frac{2n\ell(1-\theta)}{1-\ell} > n\theta$. Therefore

$$R_{\hat{\theta}_3}(\theta) < \frac{\theta(1-\theta)}{n} = R_{\hat{\theta}_1}(\theta)$$

and hence $\hat{\theta}_1$ is inadmissible.

3. <u>The Poisson Distribution</u>. Consider the Poisson density

$$f(x,\lambda) = \frac{e^{-\lambda}\lambda^x}{x!}, \quad x = 0, 1, 2, \ldots \quad . \tag{4}$$

Let $x_1, \ldots, x_n$ be a random sample from a Poisson distribution. Let $\hat{\lambda}_1 = \sum_{i=1}^{n} x_i/n$. $\hat{\lambda}_1$ is a U.M.V.U. estimator of λ with risk $R_{\hat{\lambda}_1}(\lambda) = \lambda/n$. Consider the estimator $\hat{\lambda}_2$ of the form $\hat{\lambda}_2 = k\hat{\lambda}_1$. The value of k which minimizes the mean square error is easily seen to be

$$k = \frac{\lambda^2}{\lambda^2 + \lambda/n} . \tag{5}$$

Therefore an estimator of the form

$$\hat{\lambda}_3 = \frac{\ell}{\ell + \sqrt{\ell}/n} \hat{\lambda}_1 \qquad \ell \ge 0 \tag{6}$$

is the best (in the mean square sense) estimator of λ which is a multiple of $\hat{\lambda}_1$ at the parameter value $\lambda = \sqrt{\ell}$. The estimators $\hat{\lambda}_3$ are an infinite family of admissible estimators. It is interesting to see that the U.M.V.U. estimator is best only at the parameter values $\lambda = \infty$ or $\lambda = 0$. Suppose we have prior information that $\lambda \le \ell$.

Theorem 2. If we have prior information that for the Poisson density that $\lambda \le \ell$ then

$$\lambda_3 = \left[\ell/\ell + \frac{\sqrt{\ell}}{n}\right]\hat{\lambda}_1 \tag{7}$$

is an estimator with uniformly smaller mean square error that $\hat{\lambda}_1$ and therefore $\hat{\lambda}_1$ is inadmissible.

Proof.

$$\text{m.s.e. of } \hat{\lambda}_3 = \lambda \left[\frac{\ell^2 + \frac{\ell\lambda}{n^2}}{\ell^2 + \frac{2\ell^{3/2}}{n} + \frac{\ell^2}{n^2}}\right]$$

$$< \lambda = R_{\hat{\lambda}_1}(\lambda)$$

if $\lambda \le \ell$.

4. The Normal Distribution.

Case 1. σ^2 Known.

Consider an estimator of the mean μ normal distribution with variance one. The U.M.V.U. estimator $\hat{\mu}_1$ of the mean is $\bar{x}$ with variance $1/n$. The value of k which minimizes the mean square error among all estimators of the form $k\hat{\mu}_1$ is

$$K = \frac{\mu^2}{1/n + \mu^2} \,. \tag{8}$$

Therefore an estimator of the form

$$\hat{\mu}_2 = \frac{\ell}{1/n + \ell}\,\overline{x} \text{ where } \ell \geq 0 \tag{9}$$

is the best estimator which is a multiple of $\hat{\mu}_1$ at the parameter values $\mu^2 = \ell$. It is interesting to note that the U.M.V.U. estimator is best only at the parameter value ∞. Every one of the above estimators is admissible.

Suppose we have information that the mean is bounded, that is $\mu^2 \leq \ell$.

<u>Theorem 3</u>. If we have prior information that $\mu^2 < \ell$ then $_2$ is an estimator with uniformly smaller mean square error than $\hat{\mu}_1$ and therefore $\hat{\mu}_1$ is inadmissible.

<u>Proof</u>.

$$\text{m.s.e. of } \hat{\mu}_2 = \frac{\ell^2/n + \mu^2/n^2}{\ell^2 + 2\ell/n + 1/n^2}$$

$$= 1/n \left[\frac{\ell^2 + \mu^2/n^2}{\ell^2 + 2\ell/n + 1/n^2}\right]$$

$$< 1/n = R_{\hat{\mu}_1}(\mu) \text{ if } \mu^2 \leq \ell.$$

Case 2. σ^2 Unknown.

With the variance unknown, $\overline{x} = \hat{\mu}_1$ is the U.M.V.U. estimator of μ with variance σ^2/n. The value of k which minimizes the mean square error among all estimators of the form $k\hat{\mu}_1$ is

$$k = \frac{\mu^2}{\sigma^2/n + \mu^2} = \frac{1}{\frac{1}{ns^2} + 1} \text{ where } S^2 = \frac{\mu^2}{\sigma^2} . \tag{10}$$

Consider an estimator of μ

$$\hat{\mu}_2 = \frac{1}{1/(n\ell) + 1} \hat{\mu}_1 . \tag{11}$$

The estimator $\hat{\mu}_2$ is best among estimators of the form k_1 along the lines $\ell\sigma^2 = \mu^2$ in the parameter space.

<u>Theorem 4</u>. Suppose we have prioir information that $\frac{\mu^2}{\sigma^2} \leq \ell$ then $\hat{\mu}_2$ is an estimator with uniformly smaller mean square error than $\hat{\mu}_1$ and hence $\hat{\mu}_1$ is inadmissible.

<u>Proof</u>.

$$\text{m.s.e. of } \hat{\mu}_3 = \frac{1}{n} \frac{\ell^2\sigma^2 + \mu^2/n}{\ell^2 + \frac{2\ell}{n} + 1/n^2} = \frac{\sigma^2}{n} \left[\frac{\ell^2 + \frac{\mu^2}{\sigma^2}\frac{1}{n}}{\ell^2 + \frac{2\ell}{n} + \frac{1}{n^2}}\right]$$

$$< \frac{\sigma^2}{n}$$

if $\frac{\mu^2}{\sigma^2} \leq \ell$.

5.1. <u>The Bivariate Normal Distribution</u>.

Case 1. Covariance Matrix I.

Consider a bivariate normal with variance-covariance matrix I and mean vector unknown. The U.M.V.U. estimator of $\vec{\mu} = (\mu_x, \mu_y)$ is $\hat{\mu}_1 = (\bar{X}, \bar{Y})$. It has been shown to be admissible. The value of k which minimizes the mean square among all estimators of the form $k\hat{\mu}_1$ is

$$k = \frac{||\vec{\mu}||^2}{(2/n) + ||\vec{\mu}||^2} . \tag{12}$$

The estimator

$$\hat{\mu}_2 = \frac{\ell}{(2/n) + \ell} \hat{\mu}_1 \tag{13}$$

is best in the mean square sense among estimators of the form $k\hat{\mu}_1$ for points on the sphere $\mu_x^2 + \mu_y^2 = \ell$ in the parameter space. Again the U.M.V.U. estimator appears best only at the points in the neighborhood of the point at infinity.

Theorem 5. If $||\vec{\mu}|| \le \ell$, $\ell > 0$ then $\hat{\mu}_2$ is an estimator with uniformly smaller mean square error than μ_1 and hence μ_1 is inadmissible.

Proof.

$$\text{m.s.e. of } \hat{\mu}_2 = \frac{2}{n} \frac{\ell^2 + \frac{||\vec{\mu}||^2}{n}}{\ell^2 + \frac{4\ell}{n} + \frac{4}{n^2}} < \frac{2}{n} = R_{\hat{\mu}_1}$$

if $||\vec{\mu}||^2 \le \ell$.

Case 2. Covariance matrix I σ^2, σ^2 Unknown.

The U.M.V.U. estimator for the mean is again $\hat{\mu}_1 = (\bar{X}, \bar{Y})$ with variance $2\sigma^2/n$. The value of k which minimizes the mean square error among all estimators of the form $k\hat{\mu}_1$ is

$$k = \frac{1}{\frac{2}{nS^2} + 1} \text{ where } S = \frac{||\vec{\mu}||^2}{\sigma^2}. \tag{14}$$

The estimator $\hat{\mu}_2 = k\hat{\mu}$ has smallest mean square error for points in the parameter space $\frac{||\vec{\mu}||}{\sigma^2} = \ell$.

Theorem 6. If we have prior information that $S^2 \leq \ell$ with $\ell > 0$ then $\hat{\mu}_2$ is an estimator with uniformly smaller mean square error than $\hat{\mu}_1$ and therefore $\hat{\mu}_1$ is inadmissible.

Proof.

$$\text{m.s.e. of } \hat{\mu}_2 = \frac{2\sigma^2}{n}\left[\frac{(n\ell)^2 + 2\frac{||\mu||^2}{\sigma^2}n}{(n\ell)^2 + 4\ell n + 4}\right] < \frac{2\sigma^2}{n}$$

if $\frac{||\vec{\mu}||^2}{\sigma^2} \leq \ell$.

6. The Negative Exponential Distribution. Let $x_{(1)}, \ldots, x_{(n)}$ be the order statistics of a sample of size n from

$$f(x, \mu, \sigma) = 1/\sigma \exp - (x-\mu)/\sigma \quad (x, \sigma > 0) \tag{12}$$

$$= 0 \text{ elsewhere.}$$

Let $Z = nx_{(1)}$ and $Y = 1/n \sum_{i=2}^{n} (x_i - x_{(1)})$. The distribution of $Z - n\mu$ is $\Gamma(1,\sigma)$ and the distribution of Y is $\Gamma(n-1, \sigma)$. The admissible U.M.V.U. estimator $\hat{\mu}_1$ for μ is $Z/n - Y/n(n-1)$. The estimator $\hat{\mu}_2$ which has the smallest mean square error among estimators of the form $k\hat{\mu}_1$ is the one with

$$k = \frac{\mu^2}{\frac{\sigma^2}{n(n-1)} + \mu^2} = \frac{1}{\frac{1}{S^2(n)(n-1)} + 1} \quad \text{where}$$

$$S^2 = \frac{\mu^2}{\sigma^2} . \tag{13}$$

Consider an estimator

$$\hat{\mu}_3 = \frac{1}{\frac{1}{n(n+1)\ell} + 1} \hat{\mu}_1 \quad \text{where } 0 < \ell . \tag{14}$$

The estimator is best in the mean square sense among estimators which are a multiple of $\hat{\sigma}_1$ along the lines $\ell\sigma^2 = \mu^2$ in the parameter space.

<u>Theorem 7</u>. Suppose we have prior information that $\frac{\mu^2}{\sigma^2} \leq \ell$ then $\hat{\mu}_3$ is an estimator with uniformly smaller mean square error than $\hat{\mu}_1$ and hence $\hat{\mu}_1$ is inadmissible.

<u>Proof</u>.

$$\text{m.s.e. of } \hat{\mu}_3 = \left[\sigma^2/n(n-1)\right] \frac{n^2(n-1)^2\ell^2 + n(n-1)\mu^2/\sigma^2}{n^2(n-1)^2\ell^2 + 2n(n-1)\ell + 1}$$

$$< \frac{\sigma^2}{n(n-1)} = R_{\hat{\mu}_1} \quad \text{if } \mu^2/\sigma^2 \leq \ell .$$

REFERENCES

[1] Blum, J. R. and J. Rosenblatt. "On Partial a priori Information in Statistical Inference", Annals of Mathematical Statistics, 38, 1967, pp. 1671-1678.

[2] Kale, B. K., "Inadmissibility of the Maximum Likelihood Estimator in the Presence of Prior Information", Canadian Mathematical Bulletin, 13, 1970, pp. 391-393.

[3] Katz, Morris W. "Admissible and Minimax Estimates of Parameters in Truncated Spaces", Annals of Mathematical Statistics, 32, 1961, pp. 136-142.

[4] Lehmann, E. L. Notes on the Theory of Estimation, mimeographed notes recorded by Colin Blyth, University of California, Berkeley, 1950.

[5] Robbins, H. "An Empirical Bayes Approach to Statistics", Proceedings of the Fourth Berkeley Symposium, Vol. I, Berkeley and Los Angeles, University of California Press, 1956, pp. 157-163.

[6] Skibinsky, Mark Cote L. "On the Inadmissibility of Some Standard Estimates in the Presence of Prior Information", Annals of Mathematical Statistics, 33, 1962, 539,548.

NON-NULL DISTRIBUTIONS OF THE LIKELIHOOD RATIO CRITERION FOR THE SPECTRAL MATRIX OF A GAUSSIAN MULTIVARIATE TIME SERIES

B. N. Nagarsenker

U. S. Air Force Institute of Technology

ABSTRACT

Let $\underset{\sim}{\Sigma}(\omega)$ be the spectral matrix of a p-dimensional zero-mean stationary Gaussian time series $\underset{\sim}{X}'(t) = (X_1(t), X_2(2), \ldots, X_p(t))$. In this paper, we consider the test for the null hypothesis H_0: $\underset{\sim}{\Sigma}(\omega) = \underset{\sim}{\Sigma}_0(\omega)$, where $\underset{\sim}{\Sigma}_0(\omega)$ is a known matrix for all ω, against the alternative H_1: $\underset{\sim}{\Sigma}(\omega) \neq \underset{\sim}{\Sigma}_0(\omega)$ and obtain the null and non-null distributions of the likelihood ratio criterion as mixtures of incomplete beta or gamma functions. These representations are well-suited for programming on a computer to find the exact power of the test.

1. INTRODUCTION

Let $\underset{\sim}{X}'(t) = (X_1(t), \ldots, X_p(t))$be a p-dimensional stationary Gaussian multivariate time series with zero mean vector. Let $\underset{\sim}{\Sigma}(\omega)$ denote the spectral matrix of $\underset{\sim}{X}(t)$ so that

$$\underset{\sim}{\Sigma}(\omega) = ((\sigma_{jk}(\omega)),\ (j,k = 1,2,\ldots,p) \quad ,$$

where $\sigma_{jk}(\omega) = \frac{1}{2\pi} \sum_{s=-\infty}^{\infty} R_{jk}(s) e^{-is\omega}$ denotes the cross spectral density function between $X_j(t)$ and $X_k(t)$ and

$$R_{jk}(s) = E[X_j(t) \cdot X_k(t+s)]$$

denotes the corresponding cross covariance function. We assume that for each ω the hermitian matrix $\underset{\sim}{\Sigma}(\omega)$ is positive definite. Let

$$I_{jk}(\theta_m) = \frac{1}{2\pi T} \left[\sum_{t=1}^{T} X_j(t) e^{-it\theta_m}\right] \left[\sum_{s=1}^{T} X_k(s) e^{-is\theta_m}\right]^*,$$
$$j,k = 1,2,\ldots,p.$$

where $\theta_m = \frac{2\pi m}{T}$, $m = 0,1,2,\ldots, \frac{T}{2}$.

It is well known that a consistent estimator of σ_{jk} is given by (see Parzen (1966), Brillinger (1974)

$$\hat{\sigma}_{jk}(\omega) = \frac{1}{n} \sum_{m=-n_1}^{n_1} I_{jk}(\omega + \theta_m) \quad ,$$

where $n = 2n_1 + 1$, n_1 being the bandwidth parameter. This estimate $\hat{\sigma}_{jk}(\omega)$ can be alternatively written as (see Priestly, Rao and Tong (1973))

$$\hat{\sigma}_{jk}(\omega) = \frac{1}{n} \sum_{m=1}^{n} I_{jk}(\omega' + \theta_m) \quad ,$$

where $\omega' = \omega - [2\pi\ (n_1+1)]/T$. The spectral matrix $\underset{\sim}{S}(\omega)$ is then

$$\underset{\sim}{S}(\omega) = ((\hat{\sigma}_{jk}(\omega))) = \frac{1}{n} \underset{\sim}{A}^{*}, \text{ say} \quad . \qquad \ldots(1.1)$$

Goodman (1963) showed that $\underset{\sim}{A}(\omega)$ is distributed as the Complex Wishart distribution $CW(\underset{\sim}{A}; p, n, \underset{\sim}{\Sigma})$ defined by

$$CW(\underset{\sim}{A}; p, n, \underset{\sim}{\Sigma}) = (\tilde{\Gamma}_p(n))^{-1} |\underset{\sim}{\Sigma}(\omega)|^{-n} |\underset{\sim}{A}(\omega)|^{n-p} \exp(-\mathrm{tr}\,\underset{\sim}{\Sigma}^{-1}\underset{\sim}{A}) \quad , \qquad \ldots(1.2)$$

where $\tilde{\Gamma}_p(\cdot)$ is defined in James (1964). It is easy to see from (1.1) that $\underset{\sim}{S}(\omega)$ is distributed as $CW(\underset{\sim}{S}, p, n, \frac{1}{n}\underset{\sim}{\Sigma})$. The study of the structures of the above spectral matrix and especially testing various hypotheses concerning this matrix arise in the analysis of the data in numerous areas, such as the vibrations of the airframe structures, meteorological forecasts and signal detection (see Hannan (1970), Liggett (1972, 1973), Priestley, Rao and Tong (1973), Brillinger (1974) and Krishnaiah (1976)).

In this paper, we consider the problem of testing the hypothesis $H_o: = \underset{\sim}{\Sigma}(\omega) = \underset{\sim}{\Sigma}_O(\omega)$, where $\underset{\sim}{\Sigma}_O(\omega)$ is a known matrix for all ω against the alternative $H_1: \underset{\sim}{\Sigma}(\omega) \neq \underset{\sim}{\Sigma}_O(\omega)$. We shall obtain the h^{th} moment of the likelihood ratio criterion and use these moments to derive some representations of the non-null distributions of the test statistic. These are easily programmable on a computer to obtain the exact power as well as the percentage points to any degree of accuracy.

2. SOME PRELIMINARIES

The following results and definitions are needed in the subsequent sections. The Mellin integral transform of a function f(x) of a real variable x, defined only for x > 0 is

$$M\{f(x)|s\} = E(x^{s-1}) = \int_0^\infty x^{s-1} f(x)dx \quad , \qquad \ldots(2.1)$$

where s is any complex variate. Under suitable restrictions (Titchmarsh (1948)) satisfied by all density functions considered in this paper, there is an inverse formula or inverse Mellin transform

$$f(x) = (2\pi i)^{-1} \int_{c-i\infty}^{c+i\infty} x^{-s}\{Mf(x)|s\}ds \qquad \ldots(2.2)$$

valid almost everywhere. A path of integration is any line parallel to the imaginary axis and lying within the strip of analycity of $M\{f(x)|s\}$.

Lemma 1. Let

$$\phi(t) = \int x^t \, p(x)dx$$

be the moment function of a random variable x with the distribution law p(x). If

$$\phi(t) = \underset{\sim}{O}(t^{-k}) \qquad \ldots(2.3)$$

with real part of t tending to ∞, then $\phi(t)$ can be expanded as a factorial series of the form

$$\phi(t) = \Sigma_{n=0}^{\infty} A_n \, \Gamma(t+a)/\Gamma(t+k+n+a), \qquad \ldots(2.4)$$

a being any arbitrary non-negative constant (see Nair (1940) .

Lemma 2. Let the asymptotic series $\Sigma_{j=1}^{\infty} \alpha_j x^j$ converge to the function g(x) in the neighborhood of x = 0 (or be its asymptotic expansion when x = 0). We then have

$$e^{g(x)} = 1 + \Sigma_{j=1}^{\infty} \beta_j x^j \quad , \qquad \ldots(2.5)$$

where the coefficients β_j satisfy the recurrence relation

$$\beta_j = \frac{1}{j} \; \Sigma_{k=1}^{j} \; k \, \alpha_k \, \beta_{j-k}, \; \beta_o = 1 \qquad \ldots(2.6)$$

(see Kalinin and Shalaevskii (1971).

Consider now the test for the null hypothesis H_0: $\Sigma(\omega) = \Sigma_0(\omega)$, where $\Sigma_0(\omega)$ is a known matrix against the alternative H_1: $\Sigma(\omega) \neq \Sigma_0(\omega)$. Proceeding as in Anderson (1958, p. 264), it can be shown that the likelihood ratio criterion is

$$\lambda = (e/n)^{pn} \, |A \, \Sigma_0^{-1}|^{n} \, \operatorname{etr}(-A \, \Sigma_0^{-1}) \quad , \qquad \ldots(2.7)$$

where, for convenience, we have suppressed ω and written A for $A(\omega)$, etc. Alternatively λ may be expressed as

$$\lambda = (e/n)^{pn} \, |A|^{n} \operatorname{etr}(-A), \qquad \ldots(2.8)$$

where $A \sim CW(A, p, n, \Sigma_1)$, $\Sigma_1 = \Sigma \, \Sigma_0^{-1}$.

Lemma 3. Let Z : pxp be a complex symmetric matrix whose real part is positive definite and S: pxp be a hermitian matrix. Then

$$\int_{S = S^* > 0} \exp(-\operatorname{tr} Z S) \; |S|^{a-p} \; dS = \tilde{\Gamma}_p(n) \; |Z|^{-n} \qquad \ldots(2.9)$$

(see eq. 94 of James (1964)).

Lemma 4. The h^{th} moment of the statistic λ defined in (2.8) is given by

$$E(\lambda^h) = (e/n)^{pnh} \left(\frac{|\Sigma_1|^{h}}{|I + h \, \Sigma_1|^{1+h}} \right)^{n} \frac{\tilde{\Gamma}_p(n+nh)}{\tilde{\Gamma}_p(n)} \qquad \ldots(2.10)$$

Proof: $E(\lambda^h) = \int_{A = A^* > 0} CW(A, p, n, \Sigma_1) \, . \, \lambda^h \, . \, dA$

$$= (e/n)^{pnh} \frac{|\Sigma_1|^{-n}}{\tilde{\Gamma}_p(n)} \int_{A = A^* > 0} |A|^{n+nh-p} \operatorname{etr}\{-(\Sigma_1^{-1} + hI)A\} . \, dA$$

Using Lemma 3, the result follows .

Lemma 5. The following identity is true:

$$|\underset{\sim}{I} + \frac{h}{n} \underset{\sim}{\Sigma}_1|^{-(h+n)}$$

$$= (1 + \frac{h}{n})^{-p(h+n)} \, |\underset{\sim}{\Sigma}_1|^{-(h+n)} \, |\underset{\sim}{I} - (1+\frac{h}{n})^{-1} (\underset{\sim}{I} - \underset{\sim}{\Sigma}_1^{-1})|^{-(h+n)}$$

$$= (1 + \frac{h}{n})^{-p(h+n)} \, |\underset{\sim}{\Sigma}_1|^{-(h+n)} \, \Sigma_{k=0}^{\infty} \Sigma_K \, \frac{(h+n)_K \, \tilde{C}_K(\underset{\sim}{M})}{(1 + \frac{h}{n})^k \, k!}, \qquad \ldots(2.11)$$

where $M = \underset{\sim}{I} - \underset{\sim}{\Sigma}_1^{-1}$ and $\tilde{C}_K(\cdot)$ is the zonal polynomial as defined in James (1964). This is valid since h can be chosen so that $|1 - ch \max \underset{\sim}{\Sigma}_1^{-1}| < 1 + \frac{h}{n}$.

Lemma 6. The following expansion for the gamma function holds:

$$\log \Gamma(x+h) = \log (2\pi)^{\frac{1}{2}} + (x+h-1/2)\log x - x$$

$$- \sum_{r=1}^{m} (-1)^r \frac{B_{r+1}(h)}{r(r+1)x^r} + R_{m+1}(x),$$

where $R_m(x)$ is the remainder such that $|R_m(x)| \leq \frac{\theta}{|x^m|}$, θ being a constant independent of x and $B_r(h)$ is the Bernoulli polynomial of degree r and order one.

3. NON-NULL DISTRIBUTION OF λ AS A MIXTURE OF INCOMPLETE BETA FUNCTIONS

In this section, we shall derive the non-null distribution of $L = \lambda^{\frac{1}{n}}$, where λ is given in (2.8). Using (2.10), the h^{th} moment of L under the alternative hypothesis is

$$E(L^h) = E(\lambda^{\frac{h}{n}})$$

$$= (e/n)^{ph} \frac{\tilde{\Gamma}_p(n+h)}{\tilde{\Gamma}_p(n)} \, |\underset{\sim}{\Sigma}_1|^h \cdot |\underset{\sim}{I} + \frac{h}{n} \underset{\sim}{\Sigma}_1|^{-(h+n)}, \qquad \ldots(3.1)$$

where $\Sigma_1 = \underset{\sim}{\Sigma}\,\underset{\sim}{\Sigma}_0^{-1}$. Using the inverse Mellin transform (see (2.2)), the density function of L is given by

$$f(L) = \{\tilde{\Gamma}_p(n)\}^{-1} (2\pi i)^{-1} .$$

$$\int_{c+i\infty}^{c+i\infty} L^{-h-1} (e/n)^{ph} \; \tilde{\Gamma}_p(n+h) \; |\underset{\sim}{\Sigma}_1|^h \cdot |\underset{\sim}{I} + \frac{h}{n} \underset{\sim}{\Sigma}_1|^{-(h+n)} \; dh \quad \ldots(3.2)$$

We now use the identity (2.11) of Lemma 5 and write $t = n+h$ to obtain

$$f(L) = K(p,n,\underset{\sim}{\Sigma}_1, L)$$

$$\Sigma_{k=0}^{\infty} \Sigma_K \frac{n^k}{k!} \check{C}_K(\underset{\sim}{M}) \; p(L) \quad \ldots(3.3)$$

where

$$M = \underset{\sim}{I} - \underset{\sim}{\Sigma}_1 ,$$

$$p(L) = (2\pi i)^{-1} \int_{c-i\infty}^{c+i\infty} \cdot L^{-t} \phi(t) \; dt \quad \ldots(3.4)$$

$$\phi(t) = (e/t)^{pt} \; t^{-k} \prod_{\alpha=1}^{p} \Gamma(t + k_\alpha + 1 - \alpha) \quad \ldots(3.5)$$

and

$$K(p, n, \underset{\sim}{\Sigma}_1, L) = \Pi_{\alpha=1}^{p} \{\Gamma(n+1-\alpha)\}^{-1} |\underset{\sim}{\Sigma}_1|^{-n} (e/n)^{-pn} L^{n-1} .$$

By Lemma 6, $\log \phi(t)$ may be expanded as

$$\log \phi(t) = \log (2\pi)^{p/2} + \log t^{-v} + \Sigma_{r=1}^{\infty}(q_r/t_r,)$$

where the constants q_r are given by

$$q_r = (-1)^{r-1} \{ \Sigma_{\alpha=1}^{p} B_{r+1}(k_\alpha+1-\alpha) \; / \; r(r+1)\} \quad ..(3.6)$$

and $v = p^2/2$. Thus we have

$$\phi(t) = t^{-v}(2\pi)^{p/2} \{1 + \Sigma_{r=1}^{\infty}(\ell_r/t^r)\} , \quad \ldots(3.7)$$

where the coefficients ℓ_r can be recursively computed using the relations (2.6) and (3.6). In other words, the coefficients ℓ_r satisfy the recurrence relation

$$\ell_r = \frac{1}{r} \Sigma_{k=1}^{r} \; k \, q_k \, \ell_{r-k}, \; \ell_0 = 1 \quad \ldots(3.8)$$

Now from (3.7) and (3.4) we get

$$p(L) = (2\pi i)^{-1} (2\pi)^{p/2} \int_{c-i\infty}^{c+i\infty} L^{-t} t^{-v}\{1+ \Sigma_{r+1}^{\infty}(\ell_r/t^r)\} dt \quad . \qquad ...(3.9)$$

The integral on the right hand side of (3.9) can be easily computed if v is an integer and its value, by Cauchy's theorem of residues is $2\pi i$ times the sum of the residues of $L^{-t} t^{-v} (1 + \ell_r/t^r)$ at $t = 0$. This is easily seen to be

$$(2\pi i) (2\pi)^{p/2} \Sigma_{r=0}^{\infty} \{(-\log L)^{r+v-1} \ell_r/\Gamma(v+r)\}, \ \ell_0=1$$

and thus from (3.9)

$$p(L) = (2\pi)^{p/2} \Sigma_{r=0}^{\infty}\{(-\log L)^{v+r-1} \ell_r/\Gamma(v+r)\} \quad . \qquad ...(3.10)$$

Then from (3.3), the probability that L is less than any value L_0 is

$$P(L \le L_0) = K_1(p, n, \underset{\sim}{\Sigma}_1) \Sigma_{k=0}^{\infty} \Sigma_K \frac{n^k}{k!} \tilde{C}_K (\underset{\sim}{M}) \int_0^{L_0} p(L)\, dL, \qquad ...(3.11)$$

where

$$K_1(p, n, \underset{\sim}{\Sigma}_1) = \pi_{\alpha=1}^{p} \{\Gamma(n+1-\alpha)\}^{-1} |\underset{\sim}{\Sigma}_1|^{-n} (e/n)^{-pn}.$$

For computational purposes we let $u=n-1$ and

$$I_{v+r-1,u} (L_0) = \int_0^{L_0} L^u (-\log L)^{v+r-1}/\Gamma(v+r) \ dL \quad . \qquad ...(3.12)$$

Integrating (3.12) by parts, it can be easily shown that the following recurrence relation holds:

$$I_{0,u}(L_0) = L_0^{u+1}/(u+1)$$

$$I_{v+r-1,u}(L_0) = \{L_0^{u+1} (-\log L_0)^{v+r-1}/ \Gamma(v+r) + I_{v+r-2,u}(L_0)\}/(u+1) \qquad ...(3.13)$$

With this notation, (3.11) becomes

$$P(L\le L_0) = K_1(p, n, \underset{\sim}{\Sigma}_1) \Sigma_{k=0}^{\infty} \Sigma_K \frac{n^k}{k!} \tilde{C}_K(\underset{\sim}{M}).$$

$$\Sigma_{r=0}^{\infty} \ell_r I_{v+r-1,\ u}(L_0) \quad . \qquad ...(3.14)$$

It is to be noted that (3.14) holds only if $v = p^2/2$ is an integer and this representation is computationally efficient in this case. However, if v is not an integer, we can appeal to Lemma 2 since in this case $\phi(t)$ satisfies

$$(2\pi)^{-p/2} \phi(t) = \underset{\sim}{O}(t^{-v}) \quad . \qquad ...(3.15)$$

Then from Lemma 1, we can expand $(2\pi)^{-p/2}\,\phi(t)$ in the factorial series as

$$(2\pi)^{-p/2}\,\phi(t) = t^{-v}\{1 + \Sigma_{r=0}^{\infty}\,(\ell_r/t^r)\}$$

$$= \Sigma_{i=0}^{\infty}\; R_i\;\Gamma(t+a)/\Gamma(t+v+a+i) \qquad , \qquad \ldots(3.16)$$

where a is any arbitrary positive constant and can be chosen to govern the rate of convergence of the resulting series. The coefficients R_i can be explicitly determined as is done below.

Applying Lemma 6 to each of the gamma functions in (3.16) we get

$$\log\{\Gamma(t+a)/\Gamma(t+a+v+i)\} = -(v+i)\,\log t + \Sigma_{j=1}^{\infty}\,(A_{ij}/t^j)$$

where

$$A_{ij} = (-1)^{j-1}[B_{j+1}(a) - B_{j+1}(v+a+i)]\,/j(j+1) \quad . \qquad \ldots(3.17)$$

Thus we have

$$\Gamma(t+a)/\Gamma(t+v+a+i) = t^{-(v+i)}\{1 + \Sigma_{j=1}^{\infty}(C_{ij}/t^j)\} \quad , \qquad \ldots(3.18)$$

where by Lemma 2 and (3.17), C_{ij} can be recursively computed. Using (3.18) on the right hand side of (3.16) we get

$$t^{-v}\{1 + \Sigma_{r=1}^{\infty}\,(\ell_r/t^r)\} = \Sigma_{i=0}^{\infty}\,t^{-(v+i)}\,R_i\{1 + \Sigma_{j=1}^{\infty}(C_{ij}/t^j\} \quad . \qquad \ldots(3.19)$$

Equating the coefficients of like powers of t on both sides of (3.19), it is easy to check the following explicit relations to determine R_i:

$$\Sigma_{j=0}^{\ell}\,R_{i-j}C_{i-j\,j} = \ell_i\;\;(i=1,2,3\ldots) \qquad \ldots(3.20)$$

where $R_0 = 1$ and $C_{i0} = 1$.

Now using (3.16) in (3.9) and noting that term by term integration is valid since a factorial series is uniformly convergent in a half-plane (see Doetch (1971)), we have

$$p(L) = (2\pi)^{p/2}\,\Sigma_{j=0}^{\infty}\,R_j(2\pi i)^{-1}\;\int_{c-i\infty}^{c+i\infty}\;L^{-t}\;\{\Gamma(t+a)/\Gamma(t+a+v+j)\}\;dt \;, \quad \ldots(3.21)$$

We now use the well-known integral (Titchmarch, 1948)

$$(2\pi i)^{-1} \int_{c-i\infty}^{c+i\infty} x^{-s} \{\Gamma(s+a)/\Gamma(s+a+v+j)\}\, ds = \frac{x^{a}\,(1-x)^{v+j-1}}{\Gamma(v+j)},$$

and obtain

$$p(L) = (2\pi)^{p/2} \Sigma_{j=0}^{\infty}\; R_j\; L^{a}(1-L)^{v+j-1}/\Gamma(v+j).$$

Then from (3.3), we have the following exact noncentral c.d.f of L as a mixture of incomplete beta functions:

$$P(L \le L_0) = K_1(p,\, n,\, \underset{\sim}{\Sigma}_1)\; \Sigma_{k=0}^{\infty} \Sigma_K \frac{n^k}{k!}\; \tilde{C}_K (\underset{\sim}{M}) \;.$$

$$\Sigma_{i=0}^{\infty} D_i\; B_{L_0}\, (n+a\;,\; v+i)/\Gamma(v+i), \qquad \ldots(3.22)$$

where

$$D_i = B(n+a,\; v+i)\; R_i$$

and

$$B_x(p,q) = \{B(p,q)\}^{-1} \int_0^x x^{p-1}\,(1-x)^{q-1}\, dx$$

is the incomplete beta function.

As a particular case, putting $\underset{\sim}{\Sigma} = \underset{\sim}{\Sigma}_0$, i.e., $\underset{\sim}{M} = \underset{\sim}{0}$, we get from (3.22) the null distribution of L as the following mixture of incomplete beta functions:

$$P(L \le L_0) = K_1(p,\; n,\; \underset{\sim}{I}\;)\; \Sigma_{i=0}^{\infty} D_i'\; B_{L_0}\, (n+a,\; v+i), \qquad \ldots(3.23)$$

where D_i' is the coefficient D_i with $k_i = 0$.

4. NON-NULL DISTRIBUTION OF λ AS A MIXTURE OF INCOMPLETE GAMMA FUNCTIONS

Let $L_1 = -2q \log \lambda$, where λ is as in eq (2.8) and q is an adjustable constant which can be chosen to govern the rate of convergence of the resulting series and $0 < q < \infty$. If C(t) is the characteristic function of L_1, then from (2.10) we have

$$C(t) = (n/e)^{nqpit}\; \tilde{\Gamma}_p\, \{n(1-2qit)\}\; \{\tilde{\Gamma}_p(n)\}^{-1}$$

$$|\underset{\sim}{\Sigma}_1|^{-nqit}\; |\underset{\sim}{I} - 2qit\; \underset{\sim}{\Sigma}_1|^{-n(1-2qit)}, \qquad \ldots(4.1)$$

which, as in Section 3, can be written in the form

$$C(t) = |\underset{\sim}{\Sigma}_1|^{-n} \{\tilde{\Gamma}_p(n)\}^{-1} \Sigma_{k=0}^{\infty} \frac{\tilde{C}_K(M)}{k!} H(t) \quad . \qquad \ldots(4.2)$$

where

$$H(t) = (e/n)^{-npqit} \tilde{\Gamma}_p \{n(1-2qit), K\} (1-2qit)^{-k-pn(1-2qit)} \quad , \qquad \ldots(4.3)$$

where

$$\tilde{\Gamma}_p(a,K) = (a)_K \tilde{\Gamma}_p(a)$$

as defined in Constantine (1966).

Using Lemma 6, we obtain after some simplification

$$\log H(t) = \frac{p}{2} \log 2\pi + k \log n + pn \log(n/e)$$

$$- v \log \{n(1-2qit)\} + \Sigma_{r=1}^{\infty} Q_r (1-2qit)^{-r} \quad , \qquad \ldots(4.4)$$

where $v = p^2/2$ and

$$Q_r = (-1)^{r-1} n^{-r} \left[\Sigma_{j=1}^{p} B_{r+1}(k_j + 1 - j)\right] \{r(r+1)\}^{-1} \quad , \qquad \ldots(4.5)$$

so that

$$H(t) = (2\pi)^{p/2} n^k (n/e)^{pn} \{n(1-2qit)\}^{-v} \{1 + \Sigma_{r=1}^{p} A_r (1-2qit)^{-r}\} \quad , \qquad \ldots(4.6)$$

where the coefficients A_r can be recursively computed using (4.5) and Lemma 2.

Noting that $(1 - \beta it)^{-\alpha}$ is the characteristic function of the gamma density,

$$g_\alpha(\beta,x) = \{\beta^\alpha \Gamma(\alpha)\}^{-1} x^{\alpha-1} e^{-x/\beta}, \quad x \geq 0, \ \alpha > 0, \ \beta > 0$$

we have from (4.2) and (4.6) the density of $L_1 = -2q\log\lambda$

$$f(L_1) = K_2(p, n, \underset{\sim}{\Sigma}_1) \Sigma_{k=0}^{\infty} \Sigma_K \frac{n^k \tilde{C}_K(\underset{\sim}{M})}{k!} \quad .$$

$$\Sigma_{r=0}^{\infty} A_r n^{-v} g_{r+v}(2q, L_1), \ A_0 = 1 \qquad \ldots(4.7)$$

where

$$K_2(p, n, \underset{\sim}{\Sigma}_1) = (2\pi)^{p/2} (n/e)^{pn/2} |\underset{\sim}{\Sigma}_1|^n \pi_{a=1}^{p} \{\Gamma(n+1-a)\}^{-1} \qquad \ldots(4.8)$$

and the noncentral c.d.f of L_1 is then the following mixture of incomplete gamma functions

$$P(L_1 \geq x) = K_2(p, n, \underset{\sim}{\Sigma}_1) \sum_{k=0}^{\infty} \sum_{\kappa} \frac{n^k C_\kappa(\underset{\sim}{M})}{k!} \cdot$$

$$\sum_{r=0}^{\infty} A_r n^{-v} G_{r+v}(2q, x) \qquad \ldots(4.9)$$

where

$$G_\alpha(\beta, x) = \{\beta^\alpha \Gamma(\alpha)\}^{-1} \int_x^\infty g_\alpha(\beta, y)\, dy \quad .$$

Remarks

(1) Taking $\underset{\sim}{\Sigma} = \underset{\sim}{\Sigma}_0$, or $\underset{\sim}{M} = \underset{\sim}{0}$ in (4.9), the c.d.f of $L_1 = -2q \log \lambda$ in the central case is the following mixture of incomplete gamma functions

$$P(L_1 \geq x) = K_2(p, n, \underset{\sim}{I}) \sum_{r=0}^{\infty} A_r' n^{-v} G_{r+v}(2q, x), \qquad \ldots(4.10)$$

where A_r' is the coefficient A_r with $k_r = 0$.

(2) Taking q=1, we obtain the representation of the c.d.f of L_1 in the central case as a mixture of chi-square distributions.

The representations of the c.d.f's of the likelihood ratio criterion λ obtained in this paper enable one to compute the exact power of the tests using only the tables of zonal polynomials and tables of either the incomplete beta or gamma functions and are in a form which can be easily programmed. Further, the introduction of the adjustable constants to govern the rate of convergence and the recurrence relations (3.8), (3.13) and (3.20) are well-suited to computations of power as well as percentage points for tests of significance.

5. REFERENCES

1. ANDERSON, T.W. (1958) Introduction to Multivariate Statistical Analysis Wiley, New York.

2. BRILLINGER, D.R. (1974) Time Series: Data Analysis and Theory. Holt, Rinehart and Winston, New York.

3. CONSTANTINE, A.C. (1963). Some non-central distribution problems in multivariate analysis. Ann. Math. Statist. 34, 1270-1284.

4. DOETSCH, G. (1971) Guide to Applications of the Laplace and Z-transformations. Van Nostrand - Reinhold, New York.

5. GOODMAN, N.R. (1963). Statistical Analysis based on a certain multivariate complex Gaussian distribution, (An Introduction). Ann. Math. Statist., 34, 152-177.

6. HANNAN, E.J. (1970). Multiple Time Series, Wiley, New York.

7. JAMES, A.T. (1964) Distribution of matrix variates and latent roots derived from normal samples. Ann. Math. Stat., 34, 475-501.

8. KALININ, V.M. and SHALAEVSKII, O.V. (1971) Investigations in Classical Problems of Probability Theory and Mathematical Statistics: Part I., Consultants Bureau, New York.

9. KRISHNAIAH, P.R. (1976) Some recent devleopments on complex multivariate distributions. J. Multivariate Analysis, 6, 1-30.

10. LIGGETT, JR, W.S. (1972) Passive sonar: fitting models to multiple time series in Proceedings of the NATO Advanced Study Institute on Signal Processing. Academic Press, New York.

11. LIGGETT, JR., W.S. (1973) Determination of Smoothing for Spectral Matrix Estimation. Technical Report, Raytheon Company, Portsmouth, Rhode Island.

12. NAIR, U.S. (1940) Application of Factorial Series in the Study of Distribution Laws in Statistics, Sankhya, 5, p. 175.

13. PRIESTLEY, M.B., SUBBARAO, T. and TONG, H. (1973) Identification of the structure of multivariable Stochastic Systems. In Multivariate Analysis III (P. R. Krishnaiah, Ed.) Academic Press, New York.

14. TITCHMARSH, E.C. (1948) Introduction to the Theory of Fourier Integrals. Oxford University Press, London.

Probability of Destruction of a Point Target in Space

J. S. Przemieniecki

Air Force Institute of Technology
Wright-Patterson Air Force Base, Ohio

Abstract

This paper presents an analytical method for the calculation of the probability of destruction of a point target in three-dimensional space for a given aiming offset and a spherically symmetric Gaussian distribution of the probability density function. The resulting probability is presented in terms of two non-dimensional parameters expressed in terms of the aiming offset r_0, the lethal radius R, and the variance σ^2. The resulting spherical error probable is compared with the corresponding two- and three-dimensional cases, i.e. the circular and linear error probables. The limiting case of zero aiming offset is also discussed.

Introduction

When the dimensions of a target are small compared with the effective radius of the weapon within which the target can be destroyed, the target itself can be represented by a point in the mathematical model of the attack. For example, such a model may represent the case of an anti-ballistic missile (ABM) with a nuclear warhead used to destroy an incoming reentry vehicle. Here the size of the target itself is minute in relation to the lethal radius of the ABM warhead and consequently the target can be treated as a point target. Due to systematic errors which occur in any weapon system the actual aiming point (mean point of detonation) will not coincide with the target and the usual randomness characteristics of the weapon will produce the typical scatter around the mean point of detonation. The systematic error can be accounted for by specifying the aiming offset distance from the target while the randomness error can be described by the usual standard deviation in the three-dimensional probability density function.

This paper presents the analytical method for the calculation of the probability of destruction of such a point target in space for a given aiming offset and specified lethal radius. The probability density function (PDF) describing the weapon scatter in space is assumed here to be given by a three-dimensional Gaussian distribution with equal variances. The probability of target destruction is shown to depend on two non-dimensional parameters expressed in terms of the aiming offset r_0 , the weapon lethal radius R, and the standard deviation σ . Furthermore, the paper defines the spherical error probable (SEP) as a relationship between the lethal radius parameter R/σ and the aiming offset parameter r_0/σ and then compares it with the circular error probable (CEP) and the linear error probable (LEP) . The analysis includes also a discussion of the limiting case of zero aiming offset.

Evaluation of the Probability

The analysis of the probability of destruction of a point target for two-dimensional cases has been treated extensively in the past by various authors and tabulated results are available [1-6]. This paper provides a natural extension of this analysis to three-dimensional cases which may be of importance in determining the effectiveness of an ABM system. It will be assumed that the aiming offset point (i.e. the mean point of detonation) is at a distance r_0 from the target placed at the origin of coordinate axes as shown in Figure 1.

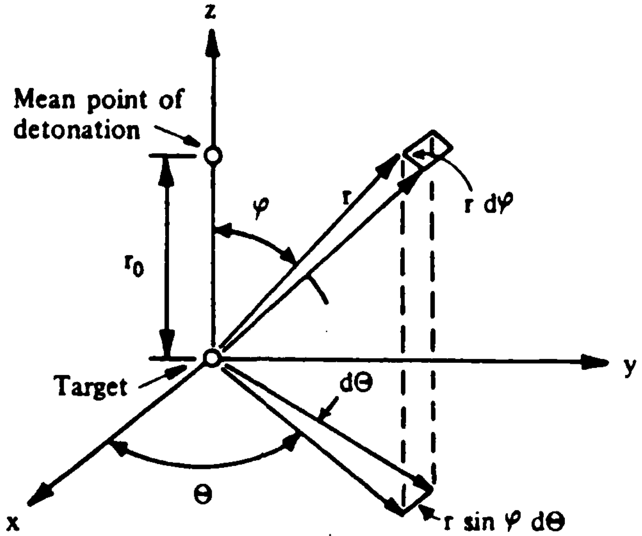

Figure 1. Target in space

The aiming offset point is assumed to lie, without any loss of generality, on the z-axis so that the three-dimensional probability density function based on equal variances σ^2 can be expressed as

$$p(x,y,z)=\frac{1}{(\sqrt{2\pi}\sigma)^3}\exp\left[\frac{-x^2}{2\sigma^2}-\frac{y^2}{\sigma^2}-\frac{(z-r_0)^2}{2\sigma^2}\right]$$

$$=\frac{1}{(\sqrt{2\pi}\sigma)^3}\exp\left[-\frac{r_0^2}{2\sigma^2}\right]\exp\left[-\frac{r^2}{2\sigma^2}+\frac{rr_0\cos\varphi}{\sigma^2}\right] \qquad (1)$$

where the relations $r^2=x^2+y^2+z^2$ and $z=r\cos\varphi$ were used.

The probability of destruction of the target is calculated from the integral

$$P=\int_0^R\int_0^\pi\int_0^{2\pi}p(x,y,z)r^2\sin\varphi\, dr\, d\varphi\, d\vartheta$$

$$=\frac{1}{(\sqrt{2\pi}\sigma)^3}\exp\left[-\frac{r_0^2}{2\sigma^2}\right]\int_0^R\int_0^\pi\int_0^{2\pi}\exp\left[-\frac{r^2}{2\sigma^2}\right]\exp\left[\frac{rr_0\cos\varphi}{\sigma^2}\right]r^2\sin\varphi\, dr\, d\varphi\, d\vartheta$$

$$=\frac{1}{\sqrt{2\pi}\sigma r_0}\int_0^R\left\{r\exp\left[\frac{-(r-r_0)^2}{2\sigma^2}\right]-r\exp\left[\frac{-(r+r_0)^2}{2\sigma^2}\right]\right\}dr \qquad (2)$$

Subsequent integration is possible with the substitution of the following variables:

$$\rho=r/[\sqrt{2}\sigma] \tag{3}$$

(The symbol ρ denotes the quantity $R/[\sqrt{2}\sigma]$ when used as an integral limit or as a parameter.)

$$\rho_0=r_0/\sqrt{2}\sigma \tag{4}$$

$$u=\rho-\rho_0 \tag{5}$$

$$v=\rho+\rho_0 \tag{6}$$

Substitution of the above variables into Eq.(2) leads to

$$P=\frac{1}{\sqrt{\pi}\rho_0}\int_{-\rho_0}^{\rho-\rho_0}(u+\rho_0)\exp(-u^2)du-\frac{1}{\sqrt{\pi}\rho_0}\int_{\rho_0}^{\rho+\rho_0}(v-\rho_0)exp(-v^2)dv \tag{7}$$

which can now be integrated. This results in an expression in terms of exponential and error functions, given by

$$P=P(R/\sigma,r_0/\sigma) \tag{8}$$

$$=\frac{1}{2\sqrt{\pi}\rho_0}\Big\{\exp\left[-(\rho+\rho_0)^2\right]-\exp\left[-(\rho-\rho_0)^2\right]$$

$$+\sqrt{\pi}\rho_0\left[erf(\rho+\rho_0)+erf(\rho-\rho_0)\right]\Big\}$$

Equation (8) is plotted in Figure 2 for a series of values of the offset parameter r_0/σ. When $r_0/\sigma=0$ (i.e. when $\rho_0=0$) then Equation (8) reduces to a special case of zero offset. Since ρ_0 appears in the denominator of Equation (8), L'Hopital's rule can be applied to obtain the limiting value when $r_0=0$. This leads to

$$P(R/\sigma,0)=\frac{-2}{\sqrt{\pi}}\rho\,exp(-\rho^2)+erf(\rho) \tag{9}$$

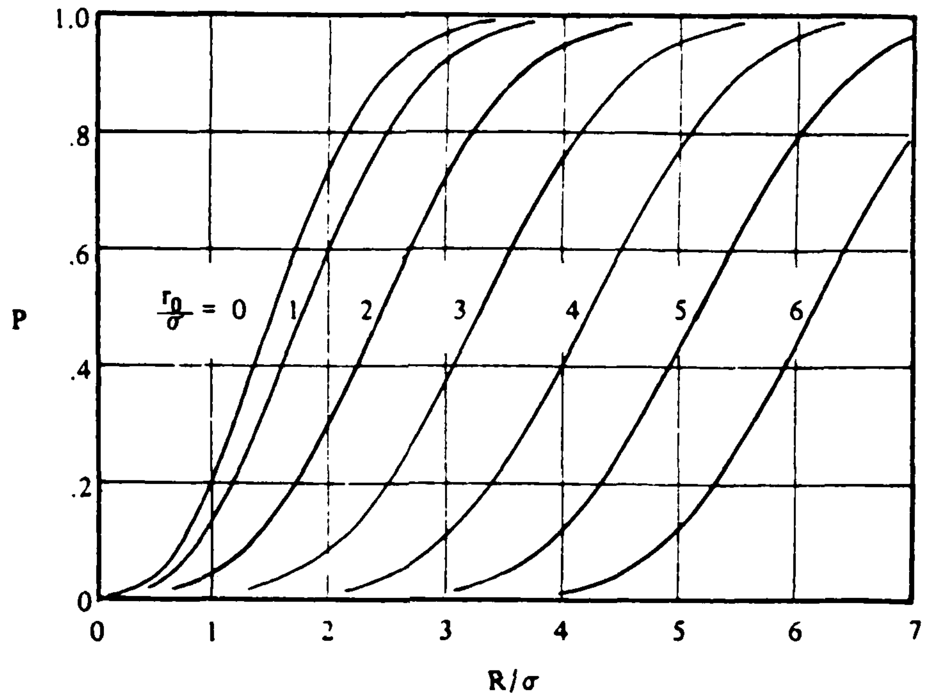

Figure 2

Probability of destruction of a point target in space for a given aiming offset r_0/σ and the lethal radius R/σ

Spherical Error Probable

For the case of zero aiming offset $r_0=0$ the Spherical Error Probable (SEP) is defined as the radius R for which 50% of all detonation points in space will fall within the radius and the remaining 50% will fall outside this radius. Thus if R represents also the lethal radius any detonations within the radius R will destroy the target. This concept can also be extended to non-zero values of r_0. This is obtained simply by equating P in Equation (8) to 1/2, so that

$$\frac{1}{2\sqrt{\pi}\rho_0}\Big\{\exp\left[-(\rho+\rho_0)^2\right]-\exp\left[-(\rho-\rho_0)^2\right] + \sqrt{\pi}\rho_0\left[erf\,(\rho+\rho_0)+erf\,(\rho-\rho_0)\right]\Big\}=1/2 \tag{10}$$

Equation (10) gives a relationship between R/σ and r_0/σ for the Spherical Error Probable. This relationship is plotted in Figure 3, which shows clearly how the lethal radius R must be increased with an increase in the offset parameter r_0/σ to achieve 0.5 (i.e. 50%) probability of target destruction. For $r_0/\sigma>1$, $R\approx r_0$, i.e. the lethal radius is approximately equal to the aiming offset.

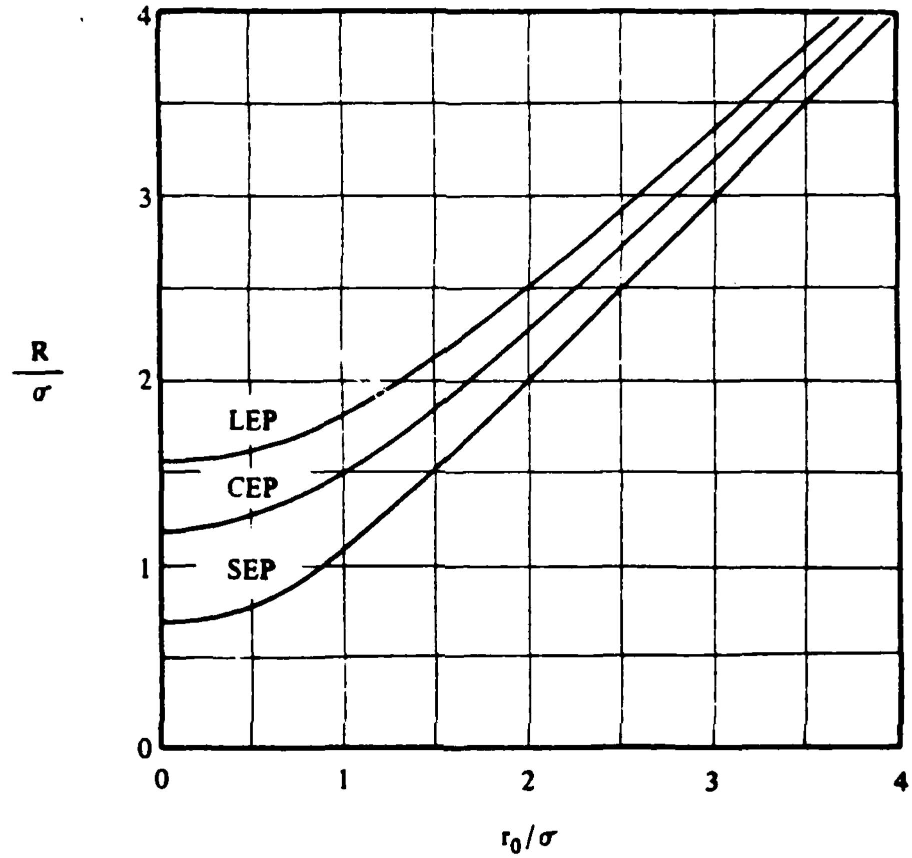

Figure 3

Variation of linear, circular, and spherical error probable with the aiming offset r_0/σ and the lethal radius R/σ.

For completeness, it is interesting to compare similar relationships for the circular and linear errors probable. Thus using results from Reference [1] it can be shown that

$$\sum_{n=1}^{\infty} g_n h_n = 1/2 \tag{11}$$

represents the required relationship for the Circular Error Probable (CEP), where

$$g_1 = 1 - exp(-\rho^2) \tag{12}$$

$$g_n = \frac{-\rho^{2(n-1)}}{(n-1)!}\exp(-\rho^2) + \frac{2}{(n-2)!} g_{n-1} \tag{13}$$

$$h_n = \frac{1}{(n-1)!}\rho_0^{2(n-1)}\exp(-\rho_0^2) \tag{14}$$

with ρ and ρ_0 defined by Equations (3) and (4), except that R and r_0 refer now to the radii in the two-dimensional impact plane containing the target.

It can be demonstrated that the corresponding relationship for the Linear Error Probable (LEP) for a point target in one-dimensional space (range) is given by

$$\frac{1}{2}\left[erf\left[\frac{R-r_0}{\sqrt{2}\sigma}\right]-erf\left[\frac{-(R+r_0)}{\sqrt{2}\sigma}\right]\right]=1/2 \tag{15}$$

where R refers to the lethal range and r_0 is the linear aiming offset. Both relationships for the circular and linear cases are also plotted in Figure 3.

Acknowledgement

The author wishes to thank Dr. David A. Lee for his assistance in programming different computer solutions presented in this paper.

References

1. Brennan, L. E. and Reed, I. S., A Recursive Method of Computing the Q-Function, IEEE Transactions on Information Theory, Vol. 11, pp. 312-313, 1965

2. Burington, R. S. and May, D. C., Handbook of Probability and Statistics with Tables, Sandusky, Ohio, Handbook Publishers, 1953

3. Groves, A. D. and Smith, E. S., Salvo Hit Probabilities for Offset Circular Targets, Operations Research, Vol. 5, pp. 222-228, 1957

4. Marcum, J. I., Table of Q-Functions, Rand Report RM-339, The Rand Corporation, Santa Monica, California, 1950

5. Rice, S. O. , Mathematical Analysis of Random Noise, Bell System Technical Journal, Vol. 24, pp. 46-156, 1945

6. Solomon, H., Distribution of the Means of a Random Two- Dimensional Set, Ann. Math. Stat., Vol 24, pp. 650-656, 1953

A NEW VARIATIONAL PRINCIPLE FOR ELASTODYNAMIC PROBLEMS WITH MIXED BOUNDARY CONDITIONS

by

Peter J. Torvik

Professor and Head

Department of Aeronautics and Astronautics

Air Force Institute of Technology

Wright-Patterson Air Force Base, Ohio 45433

Abstract

A new variational principle is presented which enables the use of a direct approach to obtaining solutions to problems in elastodynamics with mixed boundary conditions. The principle may be viewed as a modification of Hamilton's principle, in which the requirement that virtual displacements do not satisfy the displacement boundary principle to general elastodynamics. A procedure is given for using the method to determine the natural modes and frequencies of membrances and plates having mixed boundary conditions.

I. The Variational Principle

In the application of Hamilton's principle, it is necessary to seek an extremal value of the Lagrangian function over a class of admissible virtual displacements which vanish, for all time, over the portion of the boundary where the displacements are to be prescribed[1]. For many problems, finding such functions is not readily done; therefore it is of interest to investigate the possibility of extending the class of admissible functions to include functions which do not satisfy the boundary conditions on those segments of the boundary where tractions are prescribed, nor on those portions where displacements are prescribed.

This relaxation of requirements on the trial functions is precisely that permitted in the use of Reissner's principle[2], which is applicable to both the static response the the simple harmonic motion[3,4] of elastic systems. It is of interest to begin as with Hamilton's principle and to derive a somewhat more general result.

We begin by writing a Lagrangian function

$$L = U - K + A \tag{1}$$

where the strain energy, U, of an elastic material is written as a function of strains,

$$U = \int_V W(e_{ij})dV \tag{2}$$

the potential energy of conservative external forces is written as

$$A = -\int_{S_\sigma} T_i^* u_i ds - \int_V F_i u_i dV \tag{3}$$

and the kinetic energy is expressed as

$$K = \int_V \frac{1}{2} \rho \, \dot{u}_i \dot{u}_i dV \tag{4}$$

The volume of interest, V, is enclosed by the surface $S = S_u + S_\sigma$, where S_u is the portion of the boundary on which displacements are to be prescribed, and S_σ is the portion on which tractions, T_i^*, are given. The body force, F_i, is presumed to be prescribed. The customary requirement that the displacements satisfy a boundary condition

$$u_i = u_i^* \text{ on } S_u \tag{4}$$

is replaced by a constraint,

$$C_1 = \int_{S_u} \Gamma_i (u_i - u_i^*) ds \tag{5}$$

where the Γ_i are Lagrange multipliers. We assume, as in the further generalization of Reissner's principle due to Washizu[5], that the strains and displacements may be varied independently. Thus, the requirement of satisfaction of the strain displacement equations is replaced by a constraint

$$C_2 = \int_V \lambda_{ij} [e_{ij} - \frac{1}{2} (u_{i,j} + u_{j,i})] dV \tag{6}$$

where the comma denotes partial differentiation. The strains are assumed to be symmetric; thus the λ_{ij} are also.

The new functional is

$$L^* = U - K + A - C_1 - C_2 \tag{7}$$

and may be recognized as a time dependent version of the functional used in Washizu's generalization. We now seek to determine conditions under which the time integral of the modified Lagrangian function assumes a stationary value, or

$$\delta \int_{t_1}^{t_2} L^*(u_i, \dot{u}_i, e_{ij}, \lambda_{ij}, \Gamma_i)dt = 0 \tag{8}$$

with all 21 arguments of the integrand varied independently. If the trial functions, u_i, and the λ_{ij} have sufficient continuity as to permit the necessary application of the divergence theorem, and if

$$\delta u_i(t_1) = \delta u_i(t_2) = 0 \tag{9}$$

we find the vanishing of the first variation necessitates that

$$\int_{t_1}^{t_2} \int_V \{\frac{\partial W}{\partial e_{ij}} - \lambda_{ij}\}\delta e_{ij} dvdt + \int_{t_1}^{t_2} \int_V \{-\lambda_{ij} \quad + \rho \ddot{u}_i - F_i\}\delta u_i dvdt$$

$$- \int_{t_1}^{t_2} \int_V \{e_{ij} - \frac{1}{2}(u_{i,j} + u_{j,i})\}\delta\lambda_{ij} dvdt + \int_{t_1}^{t_2} \int_{S_u} (\nu_j \lambda_{ij} - \Gamma_i)\delta u_i dsdt$$

$$+ \int_{t_1}^{t_2} \int_{S_\sigma} \{\nu_j \lambda_{ij} - T_i^*\}\delta u_i dsdt - \int_{t_1}^{t_2} \int_{S_u} \{u_i - u_i^*\}\delta\Gamma_i dsdt = 0 \tag{10}$$

We recognize from the first integral that the Lagrange multipliers λ_{ij} have the physical interpretation of the components of stress in an elastic body, σ_{ij}, and from the last that the Γ_i have the physical interpretation of the components of traction, T_i, since the ν_j are the components of the normal vector at a point on the surface. Thus, three sets of Euler equations result

$$\frac{\partial W}{\partial e_{ij}} = \sigma_{ij} \text{ in } V \tag{11}$$

$$\sigma_{ij,j} + F_i = \rho \ddot{u}_i \text{ in } V \tag{12}$$

$$e_{ij} = \frac{1}{2}(u_{i,j} + u_{j,i}) \text{ in } V \tag{13}$$

and the necessary boundary conditions are seen to be

$$T_i = \nu_j \sigma_{ij} \text{ on } S = S_u + S_\sigma \tag{14}$$

$$T_i = T_i{}^* \text{ on } S_\sigma \tag{15}$$

$$u_i = u_i{}^* \text{ on } S_u \tag{16}$$

Since these are the field equations and boundary conditions of elastodynamics, we conclude that the proposed extension is appropriate, whether it be viewed as a relaxation of the class of functions to be used with Hamilton's principle, or as an extension of Reissner's principle to other than simple harmonic motions. Equation 10, it should be noted, is included in the further generalization due to Yu[6]. This dynamic variational principle differs from that of Dean and Plass[7] in that δu need not vanish on S_u.

II. An Approximate Method

Our interest here, of course, is not in deriving once again the equations of elastodynamics, but rather in developing a procedure whereby approximate solutions can be obtained for otherwise intractable problems. To do this, we return to equation 10 and make use of the identification that the Lagrange multipliers are, in fact, stresses and tractions.

We are interested in the class of problems for which a number of solutions to the field equations are readily obtained, but for which difficulties in obtaining solutions arise because of mixed boundary conditions in the form of Equations 15 and 16. We assume that a large number, N, of systems of stresses, σ_{ij}^n, and displacements u_i^n, can be found, and that each system satisfies Equation 12, and further, that these stresses satisfy an elastic constitutive relationship, Equation 11, together with strains e_{ij}^n which are derived, through Equation 13, from the displacements, u_i^n. We then take as trial functions the superpositions of such solutions, or

$$\sigma_{ij}(x,t) = \sum_{n=1}^{N} a_n \sigma_{ij}^n(x,t) \tag{17}$$

and

$$u_i(x,t) = \sum_{n=1}^{N} a_n u_i^n(x,t) \tag{18}$$

It follows that every such trial function will also satisfy the system field equations, 11-13. Tractions, T_i, may be constructed from these stresses so as to satisfy Equation 14 on each point of S.

For such trial functions, all but the last two integrals of Equation 10 are zero identically. The variational principle has thus led to the requirement that

$$\int_{t_1}^{t_2} \int_{S_\sigma} (T_i - T_i^*)\, \delta u_i ds dt - \int_{t_1}^{t_2} \int_{S_u} (u_i - u_i^*) \delta T_i ds dt = 0 \tag{19}$$

From this condition, we propose to construct an algorithm for determining the set of coefficients a_n which, for any N selected, leads to the best approximate solutions in the form of equations 17 and 18. The most general arbitrary variation within the space spanned by these N solutions may also be written as an expansion of these same N solutions, or

$$\delta\sigma_{ij} = \sum_{m=1}^{N} \delta a_m \sigma_{ij}^{m}(x,t) \tag{20}$$

$$\delta u_i = \sum_{m=1}^{N} \delta a_m u_i^{m}(x,t) \tag{21}$$

Substituting these and Equations 17 and 18 into equation 19 leads to a single equation. Since the variation must be arbitrary, however, any convenient choice of coefficients, δa_m, may be made. It is particularly convenient to make the selection:

$$\delta a_m = 0 \text{ for } m \neq p,\ m = 1,N \tag{22}$$

$$\delta a_m = 1 \text{ for } m = p,\ p = 1,N \tag{23}$$

so as to obtain a system of N equations for the N coefficients a_n, or

$$\sum_{n=1}^{N} a_n \int_{t_1}^{t_2} \left\{ \int_{S_\sigma} \nu_j \sigma_{ji}^{n} u_i^{p} ds - \int_{S_u} u_i^{n} \nu_j \sigma_{ji}^{p} ds \right\} dt$$
$$= \int_{t_1}^{t_2} \left\{ \int_{S_\sigma} T_i^* u_i^{p} ds - \int_{S_u} u_i^* \nu_j \sigma_{ji}^{p} ds \right\} dt \tag{24}$$

For any given boundary conditions, T_i^* and u_i^*, and for any selected set of solutions to the field equations, the a_n may be found and the approximate solution determined. It has been previously found [8] that static problems with mixed boundary conditions may be successfully treated in a similar manner.

The procedure may be applied to construct an approximate steady state response to a prescribed boundary excitation

$$T_i^* = \theta_i^*(s)\cos \Omega t \text{ on } S_\sigma \tag{25}$$

$$u_i^* = U_i^*(s)\cos \Omega t \text{ on } S_u \tag{26}$$

We require N solutions to the field equations, of the form

$$\sigma_{ij}^n = S_{ij}^n(\Omega,\underset{\sim}{x})\cos \Omega t \tag{27}$$

$$u_i^n = U_i^n(\Omega,\underset{\sim}{x})\cos \Omega t \tag{28}$$

Substituting these into Equation 24 yields a system of linear algebraic equations of the form

$$\sum_{n=1}^{N} a_n C_{np}(\Omega) = P_p \tag{29}$$

where

$$C_{np} = \int_{S_\sigma} \nu_j S_{ji}^n U_i^p ds - \int_{S_u} U_i^n \nu_j S_{ji}^p ds \tag{30}$$

and

$$P_p = \int_{S_\sigma} \theta_i^* U_i^p ds - \int_{S_u} U_i^* \nu_j S_{ji}^p ds \tag{31}$$

The time integrals have been eliminated from Equation 24, since the equations must be satisfied at every instant. Postmultiplying by the inverse of the array, C, completes the algorithm for computing the coefficients, a_n. For $S_u = 0$, this procedure reduces to that previously used to determine the response of an elastic strip to a time harmonic end loading[16].

In order to construct an approximate solution for the free vibration of an elastic solid with homogeneous boundary conditions, $T_i^* = 0$ on S_σ and $U_i^* = 0$ on S_u. We again require that N solutions

$$\sigma_{ij}{}^n = S_{ij}{}^n(\omega,\underset{\sim}{x})\cos\omega t \tag{32}$$

$$U_i{}^n = U_i{}^n(\omega,\underset{\sim}{x})\cos\omega t \tag{33}$$

be available. Here, the natural frequency, ω, is to be determined. Equation 24 now reduces to a set of homogeneous algebraic equations

$$\sum_{n=1}^{N} a_n C_{np}(\omega) = 0 \tag{34}$$

with C_{np} given by Equation 30. Estimates of natural frequencies, ω, arise from setting

$$\det(C_{np}) = 0 \tag{35}$$

and the corresponding mode shapes may be determined by returning the resulting value of ω to Equation 34 and computing ratios of coefficients.

We have now completed the development of a procedure whereby approximations to the forced response of elastic solids to time harmonic boundary excitations may be obtained. Approximations to the natural frequencies and the corresponding mode shapes may also be developed, even for objects of complex geometry. If the available set of solutions can be shown to be complete, convergence to an exact answer is to be expected in both cases. If the available set of solutions is merely "large", only an approximation can be anticipated.

III. Summary

A new variational principle has been developed and used to develop a general approach to the problem of determining the frequencies and mode shapes of freely vibrating elastic systems. Specific results from an application to the vibration of membranes have been given elsewhere[9,10]. These results may, of course, be immediately transferred to other physical systems having the same differential equation and boundary conditions, such as the waveguide. More recently, the method has been applied to the determination of the mode shapes and natural frequencies of vibrating plates. Specifically, the problem considered was the circular plate, clamped on a portion of the edge and free on the remainder[11]. Even though the solution algorithm requires finding, by iteration, the values of a parameter which zero the determinant of a large matrix, the computation time required was found to be substantially less than that required to obtain similar results by using the method of finite elements.

References

1. Fund, Y. C., Foundations of Solid Mechanics, Prentice Hall, 1965, p 399.

2. Reissner, E.,"On a Variational Theorem in Elasticity", Journal of Math. and Phys., Vol XXIX 1950, pp 90-95.

3. Reissner, E.,"On Variational Principles in Elasticity", Calculus of Variations and Its Applications, Proc. Sym. on Calculus of Variations, Vol VIII, American Math Soc, McGraw-Hill, 1958, pp 1-6.

4. Plass, H. J., Jr., J. H. Gaines, and C. D. Newsom, "Application of Reissner's Variational Principle to Contilever Plate Deflection and Vibration Problems", Journal of Applied Mechanics, Vol 29, March 1962, pp 127-135.

5. Washizu, K., Variational Methods in Elasticity and Plasticity, Pergamon Press, Oxford, 1968, pp 31-34.

6. Yu, Y. Y.,"Generalized Hamilton's Principle and Variational Equation of Motion in Nonlinear Elasticity with Application to Plate Theory", J. of Acoustical Society of America, Vol 36, No. 1, January 1964.

7. Dean, T. S. and Plass, H. J., "A Dynamic Variational Principle for Elastic Bodies and Its Application to Approximation in Vibration Problems", Development in Mechanics, Vol 3, No. 2, Proc. 19th Midwest Mechanics Conf, 1965, pp 107-118.

9. Van Sickel, J. R., Jr., Vibrations of Membranes and Plates with Mixed Boundary Conditions, M.S. Thesis, Air Force Institute of Technology, Wright-Patterson AFB OH, December 1978.

10. Torvik, P. J. and Van Sickel, "Natural Frequencies of Membranes Having Mixed Boundary Conditions" presented at the 95th Meeting of the Acoustical Society of America, Providence RI, May 1978.

11. Torvik, P. J., "A Variational Approach to the Dynamics of Structures Having Mixed or Discontinuous Boundary Conditions", Manuscript in preparation.

THE VALIDITY OF LINEAR VELOCITY CALCULATIONS OF LOW PRESSURE GAS FLOWS IN A FLOW TUBE

P. J. Wolf and E. A. Dorko

Department of Physics
Air Force Institute of Technology
Wright-Patterson Air Force Base, Ohio 45433

and

S. J. Davis

Air Force Weapons Laboratory
Kirtland Air Force Base, New Mexico 87117

ABSTRACT

The linear velocity and velocity profile of argon flowing in a flow tube were determined experimentally by use of a luminosity time-of-flight technique. The experiment can serve as a simple introduction to flow tubes and to velocity profile determinations in a physics or fluid mechanics laboratory. The experiment allowed the observation of a laminar flow and a comparison of linear velocity calculated from plug flow considerations with the linear, centerline velocity determined experimentally. It was found that the linear velocity was 1.62 times the plug flow (average) velocity at a flow rate of 4576.0 standard cc/min and 1.77 times the plug flow velocity at 5262.4 standard cc/min. The velocity results were compared with those predicted by the Poiseuille flow formula which governs ideal, fully developed internal flows.

INTRODUCTION

Flow tubes are relatively simple devices which can be used to determine the rates of fast reactions, to generate excited chemical species, and to study the rates of decay of the emissions from excited species. These studies can be accomplished because in the flowing gas, little mixing occurs between reactants entering and products leaving the tube. The determinations of the mechanism and kinetics of a large number of fast reactions at temperatures below $1000^{o}K$ have been done in this manner[1, 2]. In addition, with improvements in flow tube systems, high temperature reactions occurring in such systems as Fe/O_2[3] and Al/O_2[4] have been studied. Other applications of flow tubes have been reported[5, 8].

In order to perform meaningful experiments, the linear velocities of the flowing gases must be determined accurately. Linear velocities have been reported in many of the published studies[1, 8]. These velocities were needed to calculate reaction rates and to provide a basis for a correlation between various physical parameters. In general, the velocities were calculated using the plug flow assumption[8-10]. Plug flow is defined as an idealized state of flow such that, over any cross-section perpendicular to the fluid motion, the mass flow rate and the fluid properties, P, T, and ρ, remain constant. Extensive information is lacking concerning the validity of the plug flow assumption in flow tube applications where the pressure is low (4 - 10 Torr), but where the flow is still in the viscous flow regime. Swearengen[11] and Armstrong and Davis[12] have reported limited results on this problem, although it was not a main concern of their studies. The current work was conducted to develop a simple experimental method to detail the validity of the plug flow assumption in the calculation of the linear velocity of a low pressure gas in a flow tube. The linear velocity was determined experimentally and compared to calculations based on the plug flow assumption. In addition, the velocity profile was studied to determine possible deviations from plug flow. The experimental apparatus which was utilized and the technique for measuring the velocity profile are simple enough so that they could be used as a laboratory experiment in a physics or fluid flow laboratory. The experiment could introduce the students to the use of flow tubes and also could serve as a simple method of obtaining the velocity profile for a gas in laminar flow. The equipment is inexpensive and simple to operate, yet the results give a good approximation of the theoretical parabolic

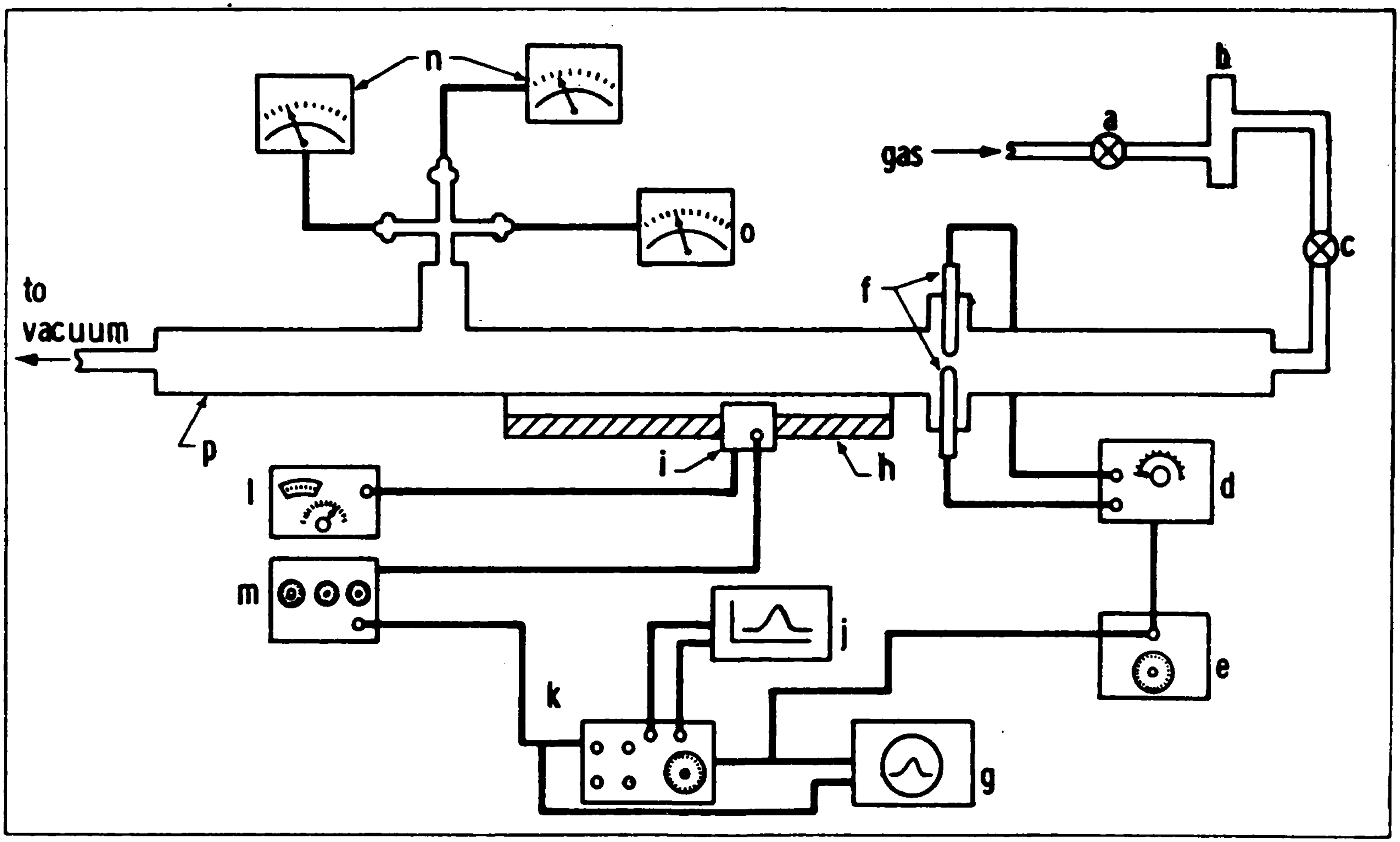

FIGURE 1: Schematic diagram of the flow tube system. The component parts are: a, needle value; b, flow meter; c, ball value; d, trigger module; e, square wave generator; f, copper electrodes; g, oscilloscope; h, optical bench; i, photomultiplier tube (PMT) system; j, x-y recorder; k, signal averager; l, PMT power supply; m, amplifier; n, vacuum gauges; o, capacitance manometer pressure gauge; p, flow tube.

velocity profile to be expected under the experimental conditions.

While standard techniques, such as pitot tubes and hotwire anemometers[13, 14] have been used in the past for velocity profile measurements, the present experiment utilized a luminosity time-of-flight technique.

A stream of argon gas was excited in a high voltage discharge in the flow tube, near the entrance. The time-of-flight of the luminous argon was determined at a series of stations downstream of the discharge by detection of the visible emission of the excited argon. The linear velocity of the flowing gas was calculated from these data. The advantage of this technique for a laboratory environment is the simplicity of the approach. Once the apparatus is assembled, simple movement of the detector along an optical bench is the only adjustment which needs to be made. By traversing the detector perpendicular to the direction of gas flow at various stations downstream at the flow tube, the development of the profile can be observed.

EXPERIMENTAL SECTION

The flow tube arrangement utilized in this experiment was based on the system described by Swearengen, Davis and Niemczyk[7, 11]. It is shown schematically in Figure 1. The flow tube was composed of sections of thick-walled pyrex glass tubing 5.1 cm I.D. joined together to form a system 162 cm in length. The tube consisted of a gas injection region, a discharge region and a test region. It was supported on an aluminum stand.

A gas flow system furnished the flow tube with a continuous supply of high purity argon (99.98%). Since the volumetric flow rate was required in order to calculate the theoretical linear velocity of the gas, this flow rate was measured using a Hastings Model A11-10K Linear Mass Flowmeter. The flow rate was controlled by a Jamesbury ball valve placed downstream from the flowmeter.

The gas entered the tube in the injection region. This 31 cm length of the flow tube, located directly upstream of the discharge region, was provided in order to obtain a reattached flow of gas prior to entry into the discharge region. Provision for the gas flow to become reattached in the flow tube becomes important when the gas feed line diameter is different from the flow tube diameter. That is, when gas is suddenly expanded as it enters a tube, a jet stream develops. Therefore, it is necessary to find a distance downstream from the inlet hole where the flow becomes reattached. In the present study, the flow tube diameter was 5.1 cm and the inlet hole diameter was 1.3 cm. For this configuration, the recirculation zone length was found to be 15 cm[15]. A section of tube approximately twice this length was used to serve as the injection region.

Once reattached flow was achieved, the gas entered the discharge region. A portion of the argon flowing between copper electrodes was ionized and excited into metastable electronic states. These states continued to emit detectable visible radiation for a considerable distance downstream, and this emission (or afterglow) served as the basis for the velocity determinations.

The discharge region was constructed with a pyrex glass cross, 20 cm in length. The cross was located directly downstream of the gas injection region. Copper electrodes, 0.32 cm in diameter, were inserted in the cross arms through 1.3 cm thich plexiglass plates. The electrodes were adjusted to provide a 1.0 cm gap perpendicular to the flow tube centerline. A high voltage arc was produced between the electrodes with an EG&G Model TM-11 30 kv trigger module. A repetitive, pulsed discharge was achieved with a 2 Hz, 20 v peak-to-peak square wave from a Wavetek Model IV voltage controlled generator.

The observation section of the test region of the flow tube, 61 cm in length, was placed directly downstream of the discharge region. An optical bench was positioned alongside this portion of the tube. The bench contained a scale graduated in cm to measure distances from the electrode to the observation point. A 1P21 photomultiplier tube (PMT), used to detect the radiation from the argon afterglow, was mounted on the optical bench. A variable slit, adjusted to a width of 0.2 cm, was placed in front of the PMT. An iris, adjusted to give a diameter of 1 cm, was placed in front of the slit. The iris allowed the photomultiplier tube to sample the radiation at different heights in the flow.

The output of the PMT was fed into a Keithly Model 427 current amplifier. The signal was then sent into a Princeton Applied Research Model TDH-9 Waveform Eductor (signal averager). Approximately 100 signals were averaged. The signal averager was triggered by the signal from the square wave generator. Therefore, the signal averager accepted signals only when the discharge was triggered. The averaged signal was then sent into a Hewlett-Packard Model 7045a X-Y Recorder. The recorder produced a curve of relative intensity vs time.

A 20 cm long pyrex glass tee was used in the test section following the observation area. This tee housed the pressure and vacuum gauges. Hastings DV-4D and DV-6 vacuum gauges were used to measure vacuum. Pressure during gas flow measured with a capacitance manometer device (MKS Baratron Type 77 Pressure Meter).

Two Welsh 17.7 CFM mechanical vacuum pumps were used to reduce the pressure in the flow tube. A pressure of 50 microns was achieved with no gas flow. A ball valve, used to retard the gas flow to provide a higher gas pressure with no change in flow rate, was placed in the line between the pumps and the flow tube.

RESULTS

A. Linear Velocity

The linear velocity of the flowing argon gas was experimentally determined at various gas pressures and flow rates by detecting the afterglow from the excited argon with the PMT. For these measurements, the PMT was positioned at various stations downstream of the electrodes. The height of the PMT system was adjusted such that a signal was detected from the flow tube centerline. The pressures, flow rates and downstream station distances for which linear velocities were calculated are listed in Table 1. The centerline signal from the flow tube was determined by traversing the PMT and the iris vertically at each station until the fastest time-of-flight of the glowing gas was obtained.

Data gathered during this operation included the distance (X) of the PMT station downstream of the electrodes and the time (t) at which the PMT detected the leading edge of the emission of the argon afterglow. An adjustment was made in the value of X in order to correct for the self-diffusion of the glowing argon. The square root of the mean square distance diffused, $\overline{(X^2)}^{\frac{1}{2}}$, was calculated using Eq (1)[16, 17]

$$\overline{(X^2)}^{\frac{1}{2}} = \sqrt{2Dt} \qquad (1)$$

where D is the diffusion coefficient of argon and t is the time-of-flight of the gas to each station. The correction amounted to less than 4% of the total distance traversed.

The linear velocity of argon was calculated by performing a linear regression analysis on the data. A linear least squares fit was computed by regressing t on X. Plots of t vs X were constructed along with the lines representing the results of the least squares analyses. This information is shown in Figure 2. The linear velocities of the gas flows were determined by inverting the slopes of the lines. The results are shown in Table II, along with the plug flow velocity calculations.

$$U_{pf} = 1.43Q\ P(ATM)/60\ P(GAS)\ A\ \text{cm/sec} \qquad (2)$$

where Q is the volumetric flow rate in standard cc/min of air, 1.43 is the conversion factor for the Hastings Mass Flowmeter to convert Q into the volumetric flow rate of argon, P(ATM) is the atomspheric pressure in torr, P(GAS) is the flowing gas pressure in torr, A is

TABLE I

EXPERIMENTAL PARAMETERS FOR LINEAR VELOCITY DETERMINATIONS

x (cm)	p (torr)	v (std cc/min)
16.9	4.2	4576.0
	6.0	4576.0
26.9	4.2	4576.0
	5.0	5262.4
	6.0	4576.0
	10.1	5262.4
31.9	5.0	5262.4
	10.1	5262.4
33.9	10.1	5262.4
37.1	4.2	4576.0
	5.0	5262.4
	6.0	4576.0
42.1	5.0	5262.4
47.0	4.2	4576.0
	5.0	5262.4
	6.0	4576.0
52.0	5.0	5262.4
56.9	5.0	5262.4
57.4	4.2	4576.0
	6.0	4576.0

TABLE II

LINEAR VELOCITY, PLUG FLOW VELOCITY, AND AVERAGE VELOCITY

Gas Pressure P(GAS) (torr)	Volumetric Flow Rate[a] $\dot{v}$ (std cc/min)	Plug Flow Velocity[b] u_{pf} (cm/sec)	Average Velocity[c] u_{AV} (cm/sec)	Experimental Linear Velocity[d] u_e (cm/sec)	u_e/u_{pf}
4.2	4576.0	663.0	664.8	1085	1.64
5.0	5262.4	637.3	638.7	1138	1.78
6.0	4576.0	464.7	465.3	738	1.59
10.1	5262.4	315.5	315.7	551	1.75

[a] Obtained from flow meter readings.

[b] Calculated using Eq (2).

[c] Calculated using Eq (4).

[d] Determined from the data shown in Figure 2.

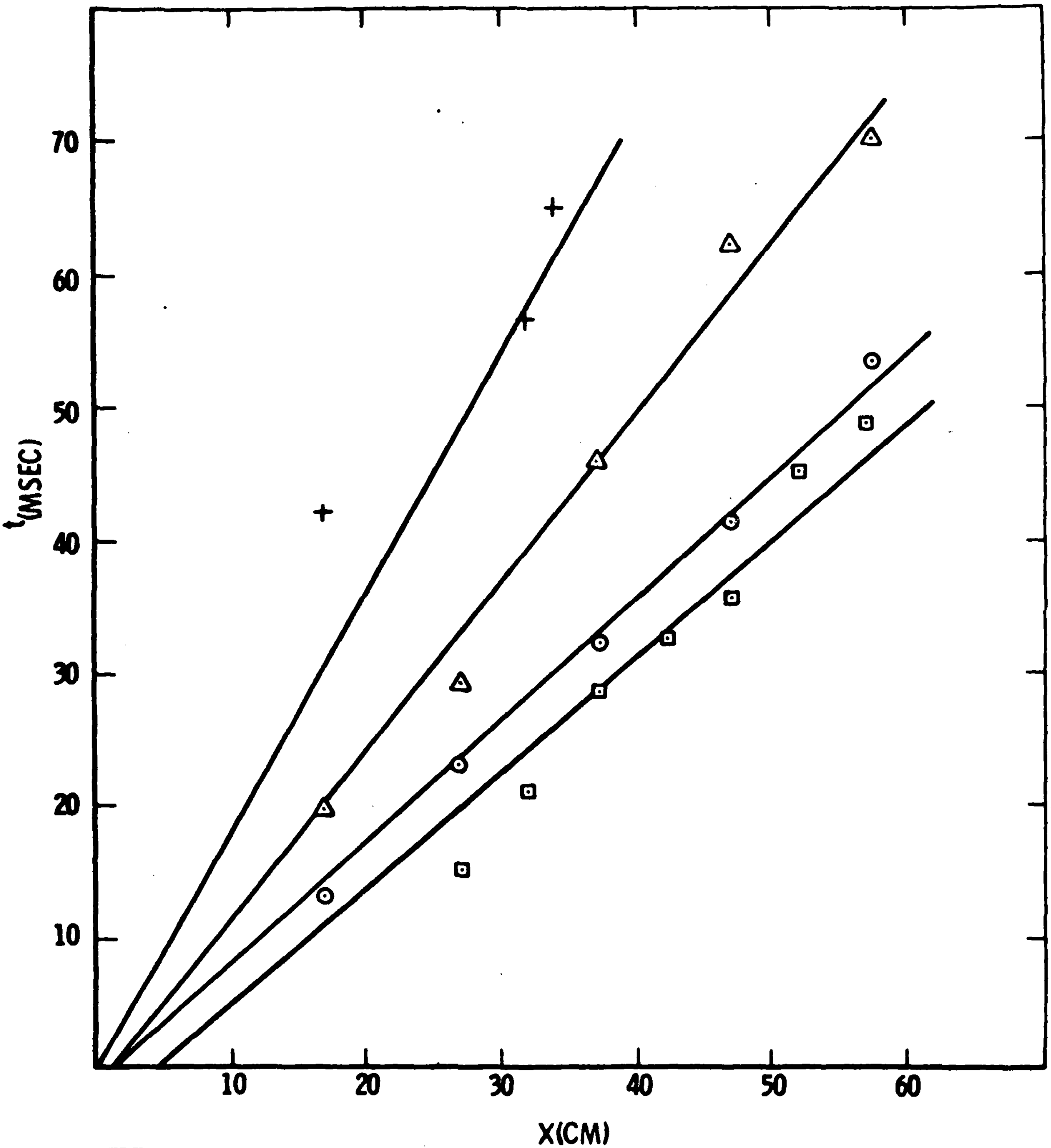

FIGURE 2: A plot of the data points for the downstream distance of the PMT station (X) versus time-of-flight (t) of the glowing argon gas. The experimental conditions are given in Table I. The data points are designated by the symbols ▣, ⊙, Δ, and + for data taken at 5.0, 4.2, 6.0, and 10.1 torr, respectively.

the cross-sectional area of the flow tube (20.27 cm^2) and 60 is the conversion factor from minutes to seconds.

B. Velocity Profile

The velocity profile of the gas flow is dependent upon the type of flow present (i.e., molecular, viscous, or intermediate). The division between these flow regimes is determined by the value of the Knudsen number [18]. In this study, the mean free path of argon at 5.0 torr was calculated to be 1.04×10^{-3} cm and the Knudsen number was 2.05×10^{-4}. Therefore, the flow is in the viscous flow region[18]. Furthermore, the Reynolds number was calculated to be 280, which showed that the flow was laminar[10] as well. Therefore, a parabolic velocity profile was predicted to form in the flow tube.

The instantaneous linear velocity of argon was determined at various heights above and below the flow tube centerline from time vs distance data. The data for these calculations were obtained at stations 28.5 cm and 35.9 cm downstream from the electrodes. These experimental velocities were then plotted against distance above and below the flow tube centerline to obtain the profile. The results are shown graphically in Figure 3. The solid parabolic curve in Figure 3 is a theoretical velocity profile characteristic of a fully developed internal flow. This profile was determined using the Poiseuille flow formula for a flow in circular cross-section[10].

$$u(y) = 2u_{AV} \, [1 - y^2/R^2)] \tag{3}$$

where y is the radial distance from the centerline and R is the radius of the tube. u_{AV} is defined in Eq (4)

$$u_{AV} = \frac{-R^2}{8\eta} \, \frac{\Delta p}{\Delta x} \tag{4}$$

where η is the viscosity and Δp is the pressure difference due to

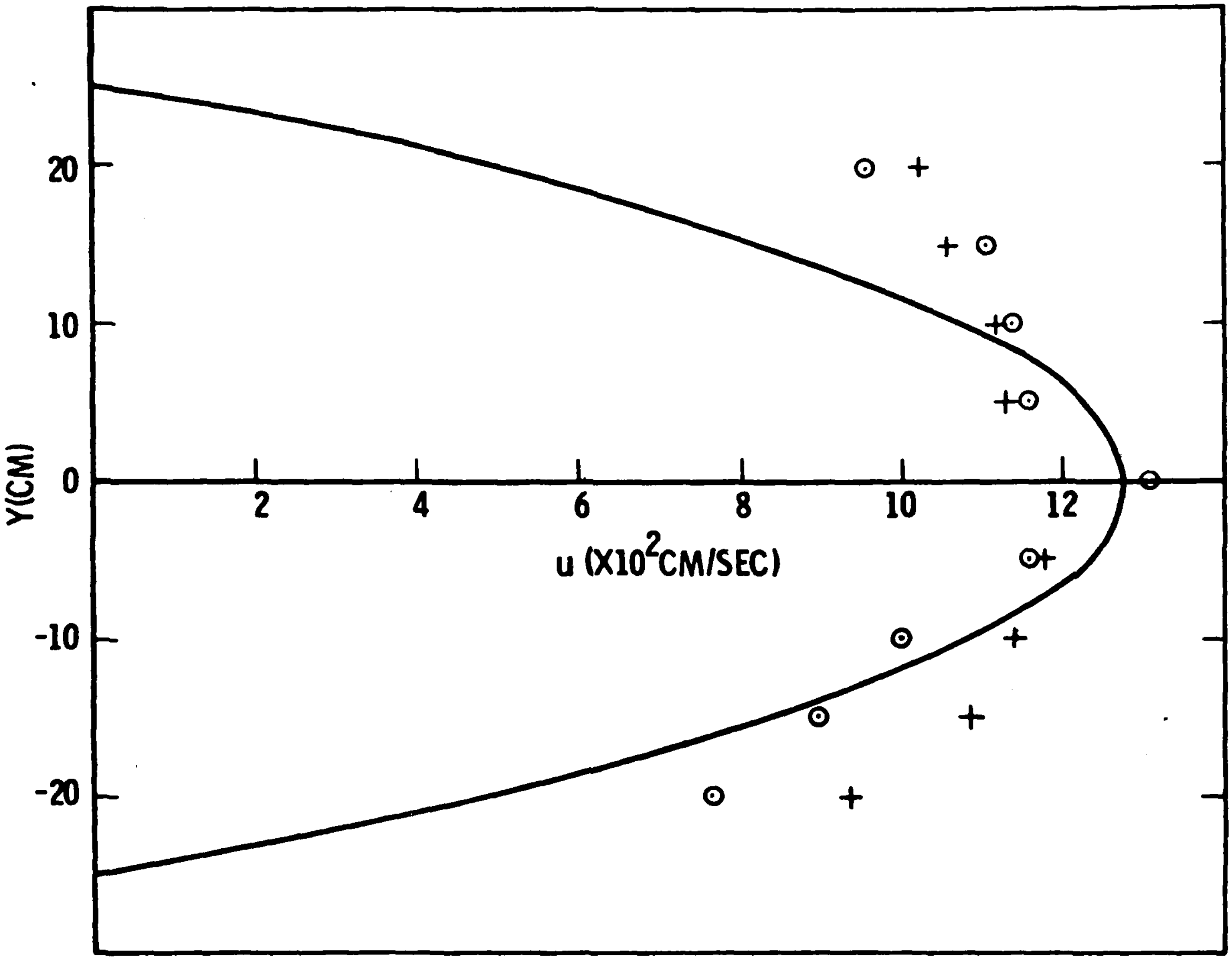

FIGURE 3: Experimental and theoretical velocity profiles at 5.0 torr. The parabolic profile was calculated using the Poiseuille flow formula. The experimental data were taken at PMT stations 28.5 cm (+) and 35.9 cm (O) downstream of the electrodes.

viscous forces over a length of tube Δx. If the pressure at one end of the tube is known, then the pressure at the other end can be calculated from Eq (5)[2]

$$P_2^2 - P_1^2 = 16F' \, L\eta \, R_0T/\pi R^4 \tag{5}$$

where F' is the flow rate in moles/sec, L is the length of the tube, R_0 is the universal gas constant, and T is the absolute temperature. For example, using for the viscosity of argon 223.7×10^{-6} poise at 296° K, a P_1 of 10.1 torr and a flow rate of 3.62×10^{-3} mole/sec, the pressure difference due to viscous forces was calculated to be 1.09×10^{-2} torr.

The experimental velocity profiles in Figure 3 revealed an approximately parabolic configuration at both stations. While the profile obtained at 35.9 cm downstream slightly more closely resembled the theoretical curve than the profile at 28.5 cm, the difference in the profiles is within experimental scatter. Therefore, the flow was considered fully developed at both downstream stations. The characteristic length for an internal flow to become fully developed was calculated using Eq (6)[9]

$$X_L = .03 \, (R_e) \, D \tag{6}$$

where X_L is the characteristic length, R_e is the Reynolds number and D is the tube diameter. The laminar development length was calculated as 42.7 cm from the point where the flow became reattached at the inlet region. Thus, the flow was fully developed at 16.7 cm downstream from the electrodes. This simple calculation was strongly supported by a numerical calculation for the same system which was performed by Rapagnani and Davis[19].

DISCUSSION

The velocity profiles of the flowing argon gas at various low pressures were parabolic. This result indicates that a fully developed laminar flow was present throughout the experiment. Based on this conclusion, a comparison can be made between the experimentally determined values for plug flow (Eq (2)) and the average velocities calculated by the use of Eqs (4) and (5). These values are reported in Table II. The correspondence between values shows that the plug flow velocity can be used as the average velocity in calculations for flow tubes when low pressure laminar flow is occurring.

The results of the linear velocity calculation along the flow tube centerline should be twice the average or plug flow velocity in the ideal case. This is evident when y is set equal to 0 in Eq (3). A comparison between the experimental linear velocity results at $y = 0$, (u_e), and the plug flow values shows that the factor of 2 is being approached, but experimentally the linear velocity is somewhat slower than predicted by theory. The discrepancy can be the result of a number of factors. Plug flow calculations do not take into account frictional effects, since this calculation is based on an ideal flow. In this study, the flow experienced frictional effects due to shearing stresses and pressure losses which caused the deviation from plug flow. Also, in the present case the frictional effects were increased when the gas flowed past the electrodes.

Based on these studies, it is concluded that a calculation of centerline velocity based on a laminar velocity profile gives a much better value than a calculation based on plug flow. If perturbations to the flow are slight, as in the present case, a correction factor of 1.6 - 1.7 applied to the plug flow value will give a good estimate of the centerline flow velocity.

REFERENCES

1. G. Porter, Ed., Progress in Reaction Kinetics, Vol 1, Pergamon Pres, New York, 1961.

2. B. A. Thrush, Science, 154, 477 (1967).

3. A. Fontjin and S. C. Kurzius, Chem. Phys. Letters, 13, 507 (1972).

4. A. Fontjin, W. Felder, and J. J. Houghton, Chem. Phys. Letters, 27, 365 (1974).

5. R. L. Brown, J. of Res., NBS, 83 1 (1978).

6. G. Dixon-Lewis, W. E. Wilson, and A. A. Westenberg, J. Chem. Phys., 44, 2877 (1966).

7. P. M. Swearengen, S. J. Davis, and T. M. Niemczyk, Chem. Phys. Letters, 55, 274 (1978).

8. S. M. Walas, Reaction Kinetics for Chemical Reactions, McGraw-Hill Book Company, Inc., New York, 1959.

9. J. M. Coulson and J. F. Richardson, Chemical Engineering, Vol 3, Pergamon Press, New York, 1971.

10. K. Denbigh, Chemical Reactor Theory, An Introduction, Cambridge University Press, New York, 1965.

11. P. M. Swearengen, "Kinetic Studies of Silicon and Germanium Oxide Reactions", PhD Dissertation, Department of Chemistry, The University of New Mexico, December 1977.

12. R. A. Davis and S. J. Armstrong, Chem. Phys. Letters, 57, 446 (1978).

13. C. F. Shoop, and G. L. Tuve, Mechanical Engineering Practice, 5th Edition, McGraw-Hill Book Company, Inc., New York, 1956.

14. J. E. A. John, and W. Haberman, Introduction to Fluid Mechanics, Prentice-Hall, Inc., Englewood Cliffs, N. J., 1971.

15. M. A. Pennucci, "Parametric Evaluation of Total Pressure Loss and Recirculation - Zone Length in a Sudden Expansion Combustor", M.S. Thesis, School of Engineering, Air Force Institute of Technology, Wright-Patterson Air Force Base OH 45433, 1974.

16. W. J. Moore, Physical Chemistry, 4th Edition, Prentice-Hall, Inc., Englewood Cliffs, N. J., 1972, pp 162-163.

17. Shyh Wang, Solid State Electronics, McGraw-Hill Book Company, Inc., New York 1966, pp 282-290.

18. A. Roth, Vacuum Technology, North-Holland Publishing Co., New York, 1976.

19. N. L. Rapagnani and S. J. Davis, Chemical Laser Branch, Air Force Weapons Laboratory, Albuquerque NM, private communication.

Unclassified

SECURITY CLASSIFICATION OF THIS PAGE

REPORT DOCUMENTATION PAGE

1a. REPORT SECURITY CLASSIFICATION: Unclassified

1b. RESTRICTIVE MARKINGS

2a. SECURITY CLASSIFICATION AUTHORITY

2b. DECLASSIFICATION/DOWNGRADING SCHEDULE

3. DISTRIBUTION/AVAILABILITY OF REPORT: Approved for public release; distribution unlimited.

4. PERFORMING ORGANIZATION REPORT NUMBER(S): AFIT-EN-TM-84-1

5. MONITORING ORGANIZATION REPORT NUMBER(S)

6a. NAME OF PERFORMING ORGANIZATION: Air Force Institute of Technology, School of Engineering

6b. OFFICE SYMBOL *(If applicable)*: AFIT/EN

7a. NAME OF MONITORING ORGANIZATION

6c. ADDRESS *(City, State and ZIP Code)*: Wright-Patterson AFB OH 45433

7b. ADDRESS *(City, State and ZIP Code)*

8a. NAME OF FUNDING/SPONSORING ORGANIZATION

8b. OFFICE SYMBOL *(If applicable)*

9. PROCUREMENT INSTRUMENT IDENTIFICATION NUMBER

8c. ADDRESS *(City, State and ZIP Code)*

10. SOURCE OF FUNDING NOS.

PROGRAM ELEMENT NO.	PROJECT NO.	TASK NO.	WORK UNIT NO.

11. TITLE *(Include Security Classification)*: A Festschrift of Technical Papers Presented to W. S. Ericksen (U)

12. PERSONAL AUTHOR(S): Brian W. Woodruff, Capt, USAF; editor - see item 19 for authors of papers

13a. TYPE OF REPORT	13b. TIME COVERED	14. DATE OF REPORT (Yr., Mo., Day)	15. PAGE COUNT
Technical Memorandum	FROM ______ TO ______	1984 January	87

16. SUPPLEMENTARY NOTATION

Approved for public release: IAW AFR 190-17.
Lynn Wolaver 14 May 84
LYNN E. WOLAVER
Dean for Research and Professional Development
Air Force Institute of Technology (ATC)
Wright-Patterson AFB OH 45433

17. COSATI CODES

FIELD	GROUP	SUB. GR.

18. SUBJECT TERMS *(Continue on reverse if necessary and identify by block number)*: Key words - see reverse.

19. ABSTRACT *(Continue on reverse if necessary and identify by block number)*

This volume contains eight technical papers written by colleagues of Wilhelm Ericksen in honor of his 30 years of service on the faculty of the Air Force Institute of Technology. The following is a list of titles and authors of the papers in the volume: "The PCT Control System Design for Sampled-Data Control Systems", by C. H. Houpis; "Asymptotic Non-Null Distribution of a Test of Equality of Exponential Populations", by R. W. Kulp and B. N. Nagarsenker; "Irrotational and Solenoidal Waves in General Coordinates", by D. A. Lee; "Some Problems of Estimation When Some Prior Information is Available", by A. H. Moore; "Non-Null Distributions of the Likelihood Ratio Criterion for the Spectral Matrix of a Gaussian Multivariate Time Series", by B. N. Nagarsenker; "Probability of Destruction of a Point Target in Space", by J. S. Przemieniecki; "A New Variational Principle for Elastodynamic Problems with Mixed Boundary Conditions", by P. J. Torvik; "The Validity of Linear Velocity Calculations of Low Pressure Gas Flows in a Flow Tube", by P. J. Wolf, E. A. Dorko and S. J. Davis.

20. DISTRIBUTION/AVAILABILITY OF ABSTRACT: UNCLASSIFIED/UNLIMITED ☒ SAME AS RPT. ☒ DTIC USERS ☐

21. ABSTRACT SECURITY CLASSIFICATION: Unclassified

22a. NAME OF RESPONSIBLE INDIVIDUAL	22b. TELEPHONE NUMBER (Include Area Code)	22c. OFFICE SYMBOL
Brian W. Woodruff	513-255-2915	AFIT/ENC

DD FORM 1473, 83 APR — EDITION OF 1 JAN 73 IS OBSOLETE.

Unclassified

SECURITY CLASSIFICATION OF THIS PAGE

Item 18 continued:

pseudo-continuous-time control system
sampled-data system
exponential populations
likelihood ratio criterion
asymptotic non-null distribution
Chi-square distributions
elastodynamic displacement fields
irrotational waves
solenoidal waves
prior information
admissible estimators
inadmissible estimators
spectral matrix
multivariate time series
target destruction probability
spherical error probable
circular error probable
linear error probable
variational principle
elastodynamic problems
boundary conditions
flow tubes
plug flow
Poiseuille flow formula

END

FILMED

DTIC